land

MDPI

Article

The Role of Soil Type in Triggering Shallow Landslides in the Alps (Lombardy, Northern Italy)

Fabio Luino [1], Jerome De Graff [2], Marcella Biddoccu [3,*], Francesco Faccini [1,4], Michele Freppaz [5], Anna Roccati [1], Fabrizio Ungaro [6], Michele D'Amico [7] and Laura Turconi [1]

1 Istituto di Ricerca per la Protezione Idrogeologica, Consiglio Nazionale delle Ricerche, Strada delle Cacce 73, 10135 Torino (TO), Italy; fabio.luino@irpi.cnr.it (F.L.); faccini@unige.it (F.F.); anna.roccati@irpi.cnr.it (A.R.); laura.turconi@irpi.cnr.it (L.T.)
2 Department of Earth & Environmental Science, California State University, M/S ST24, Fresno, CA 93740, USA; jdegraff@csufresno.edu
3 Istituto di Scienze e Tecnologie per l'Energia e la Mobilità Sostenibili, Consiglio Nazionale delle Ricerche, Strada delle Cacce 73, 10135 Torino (TO), Italy
4 Dipartimento di Scienze della Terra, dell'Ambiente e della Vita, Università di Genova, Corso Europa 26, 16132 Genova (GE), Italy
5 Dipartimento di Scienze Agrarie, Forestali e Alimentari, Università di Torino, Largo Paolo Braccini 2, 10095 Grugliasco (TO), Italy; michele.freppaz@unito.it
6 Istituto per la BioEconomia, Consiglio Nazionale delle Ricerche, Via Madonna del Piano 10, 50018 Sesto Fiorentino (FI), Italy; fabrizio.ungaro@ibe.cnr.it
7 Dipartimento di Scienze Agrarie e Ambientali—Produzione, Territorio, Agroenergia, Università degli Studi di Milano, Via Celoria 2, 20133 Milano (MI), Italy; michele.damico@unimi.it
* Correspondence: marcella.biddoccu@cnr.it or marcella.biddoccu@stems.cnr.it

Abstract: Shallow landslides due to the soil saturation induced by intense rainfall events are very common in northern Italy, particularly in the Alps and Prealps. They are usually triggered during heavy rainstorms, causing severe damage to property, and sometimes causing casualties. A historical study and analysis of shallow landslides and mud-debris flows triggered by rainfall events in Lombardy was carried out for the period of 1911–2010, over an area of 14,019 km^2. In this study, intensity–duration rainfall thresholds have been defined using the frequentist approach, considering some pedological characteristics available in regional soil-related databases, such as the soil region, the textural class, and the dominant soil typological units (STU). The soil-based empirical rainfall thresholds obtained considering the soil regions of the study area were significantly different, with a lower threshold for landslide occurrence in the soil region M1 (Alps), where soils developed over siliceous parent material, with respect to the whole study area and the soil region M2 (Prealps), where soils developed over calcareous bedrocks. Furthermore, by considering textural classes, the curves were differentiated, with coarse-textured soils found more likely to triggerlandslides than fine soils. Finally, considering both texture and main soil groups, given the same rainfall duration, the rainfall amount and intensity needed to initiate a landslide increased in the following order: "coarse-skeletal" Cambisols < Umbrisols < Podzols < "fine" Cambisols. The results of this study highlighted the relevant role of pedological conditioning factors in differentiating the activation of rainfall-induced shallow landslides in a definite region. The information on soils can be used to define more precise rainfall–pedological thresholds than empirical thresholds based solely on meteorological conditions, even when they are locally defined. This knowledge is crucial for forecasting and preventing geo-hydrological processes and in developing better warning strategies to mitigate risks and to reduce socio-economic damage.

Keywords: rainfall threshold; soil region; soil texture; soil typological units; Northern Italy

Citation: Luino, F.; De Graff, J.; Biddoccu, M.; Faccini, F.; Freppaz, M.; Roccati, A.; Ungaro, F.; D'Amico, M.; Turconi, L. The Role of Soil Type in Triggering Shallow Landslides in the Alps (Lombardy, Northern Italy). *Land* **2022**, *11*, 1125. https://doi.org/10.3390/land11081125

Academic Editors: Irene Manzella and Bouchra Haddad

Received: 16 June 2022
Accepted: 19 July 2022
Published: 22 July 2022

1. Introduction

Landslides are the most widespread and hazardous natural processes in hillslope and mountain environments around the world, which have contributed and continue to contribute to the shaping of the earth's surface. Shallow landslides/soil slips cause billions of euros in damage to physical assets and properties and thousands of casualties and evacuees each year [1–5]. The occurrence and the spatial distribution of the landslides are linked to a large range of triggering factors in a general geographical setting given by certain preconditioning and preparatory factors [6].

Slope instability is the result of a complex combination of several predisposing and causal factors, including geological, topographic, hydrological, environmental, and anthropogenic parameters [7–9]. Due to the heterogeneous spatial distribution and temporal variability of physical features, such as land use, climate, soil properties, and ground water regimes, slope failures are very difficult to model and predict [10–12]. Understanding landslide activation is essential for supporting local administrations in the improvement of efficient early warning systems and the management of the most effective strategies, which are aimed at mitigating and reducing landslide hazards and their impact on population and assets [13–17].

In particular, debris flows are a transport mechanism for debris material (usually lithoid and vegetation) that result in large amounts of material being delivered rapidly downstream [18–20]. They have destructive capabilities because of their high impact force (a function of the velocities reached and the mass in transit) enabling them to lift and carry large objects such as boulders and trees. Debris flows are also often improperly referred to as rapid landslides or shallow landslides because they can be fed by slope deposits (or eluvial-colluvial blankets) that—as a result of gravity and the fluidization of the surface soil layers—are channelled into small slope incisions or catchment/torrential beds. However, the triggering conditions for debris flows are comparable to shallow landslides [21–24]; indeed, the latter often evolve in mud and/or debris flows, especially if they are triggered on slopes for which the foot ends in a torrential bed. For this reason, these processes are often conceptually united, especially if they occur during severe rainstorms [12,25–28]. The alpine and pre-alpine districts of Lombardy are among the mountain areas in Italy with the largest number of properties and people exposed to high and very high landslide risks [28–30]. This territory has historically been affected by destructive shallow landslides and mud-debris flows, causing considerable damage to structures and infrastructures and great losses in terms of properties and human lives [25,31–35], particularly during intense rainfall events.

Nowadays, the knowledge of the physical and environmental factors influencing landslide activation within the Alpine domains is still lacking and incomplete, and few studies have investigated soil properties and their relations with failure mechanisms within these mountain areas [10,36–42].

In the literature, several empirical and physically based approaches have been proposed to define thresholds for hydrological conditions—including rainfall, soil moisture, and infiltration—that result in landslides [26,27]. Several authors have proposed different methods to identify rainfall thresholds for the possible initiation of landslides [13,14,26,27,43,44]. Most studies have only considered rainfall variables, as precipitation is recognized as the most important and easy-to-quantify landslide-triggering factor [27,45]. Different modeling approaches have been proposed to identify simple and functional empirical cause–effect correlations based on the analysis of landslides that have occurred in the past and their related rainfall values.

In most works, in relation to the difficulties of reporting thresholds based on physical data, empirical approaches are adopted to study correlations between rainfall events and landslide occurrences, particularly when the investigation is focused on the development of warning systems aimed at mitigating the possibly severe consequences and damage to property and population. These works have considered several variables to identify rainfall characteristics responsible for slope failures, such as cumulative event rainfall, intensity, duration, antecedent rainfall, and various combinations of these. Intensity–duration (ID) thresholds are the most widely used empirical thresholds for studying shallow or rapid landslides, which are usually triggered by short-duration, high-intensity precipitation [17,42,46–53]. Adopting statistical or probabilistic techniques, empirical rainfall thresholds have been generally defined for different physiographic settings, types of mass movement, and spatial scales (global, regional, local, or single catchment) [13,26,44,48,49,53–58]. Only a few empirical studies have investigated predisposing hydrological parameters, such as antecedent soil moisture content, in relation to landslide-triggering mechanism thresholds [59–64].

On the contrary, a number of studies have investigated landslide-conditioning factors, considering the lithological, hydrological, environmental, or anthropogenic parameters that predispose slopes to instability and influence the activation of mass movements [42,45,65–70]. In the literature, different mathematical models have been proposed to estimate the rainfall conditions leading to the activation of landslides, considering soil hydrological and geotechnical parameters and geomorphological features and dynamics. They are generally based on infinite slope stability analysis, with dynamic hydrologic or steady groundwater flow conditions, or on the modeling of water infiltration dynamics and groundwater pressure in soils [14,71–78]. However, physically based approaches are usually difficult to apply because of the spatial and temporal variability of geotechnical and hydrological parameters, which are complex to manage and measure [70,79].

With particular reference to the Alpine region, different empirical and mathematical methods have been proposed to investigate the conditions for the occurrence of rainfall-induced shallow landslides, since the first attempts based on mean annual precipitation (MAP) by Govi and Sorzana [80] and those based on rainfall duration and intensity [36]. More recently, using 80 years' worth of data collected in the Sondrio and Brescia Provinces, Luino et al. [81] established new empirical MAP-normalized intensity–duration thresholds for shallow landslides and mud-debris flows in the alpine and pre-alpine districts of the Lombardy region. The activation of mass movements was found to be strongly influenced by pedological and topographic properties, such as soil moisture, soil type, and slope acclivity, whereas lithology played a secondary role in triggering mechanisms, but only few studies considered both soil and rainfall information to understand the failure activation, which defines soil-based thresholds [41,42,50,82].

In this paper, we present a study carried out in the Lombardy region (Northern Italy, Figure 1) based on an empirical approach that uses a large dataset of shallow landslides that have occurred in the past, with the aim of (i) identifying the pedological properties that most significantly influence the activation of rainfall-induced landslides in the study area, (ii) defining differentiated rainfall thresholds for separated pedological domains within the study area, (iii) defining rainfall–threshold curves for the possible occurrence of shallow landslides and mud-debris flows in the mountain districts of the Lombardy region (Varese, Como, Lecco, and Bergamo Provinces), and finally (iv) comparing the rainfall thresholds based on soil domains with the rainfall regional thresholds proposed by several authors for the alpine and pre-alpine area.

Figure 1. Location of the study area: the (**A**) alpine and (**B**) pre-alpine district of the Lombardy region, with indications of administrative provinces: Varese (VA), Como (CO), Lecco (LC), Bergamo (BG), Sondrio (SO), and Brescia (BS).

2. Materials and Methods

2.1. Study Area

The study area includes the alpine and pre-alpine districts of Lombardy (Figure 1). thus the mountain areas of the following administrative provinces: Varese (VA), Como (CO), Lecco (LC), Bergamo (BG), Sondrio (SO), and Brescia (BS).According to the recent international orographic classification of the Alpine system [83], the Alps and Prealps in Lombardy are included within the North-Western, Central-, and South-Eastern Alps (Figure 1).

2.1.1. Climate

Due to its orographic configuration, the climate setting of Lombardy region has a significant spatial variability. Altitude and slope aspect, prevailing winds, and the presence of large lakes influence the rainfall regime. As reported in [84], the mean annual precipitation (MAP) values range from 800–1000 mm/y in the upper Po plain up to 2000–2300 mm/y in the pre-alpine and southern alpine belts, where rainfall can locally exceed 2400 mm/y (Figure 2). The alpine valleys are generally characterized by lower MAP values, which range from 600 mm/y in the continental Livigno district (NE) and 1800 mm/y in the Valchiavenna Valley (NW). At high elevation, winter snowfalls represent more than half of the total annual precipitation. Heavy rainfalls are frequent in the spring and autumn months [85,86] due to westerly and southerly winds, whereas summer is characterized by abundant precipitation next to mountain ridges, induced by convection and the orographic air uplift [38].

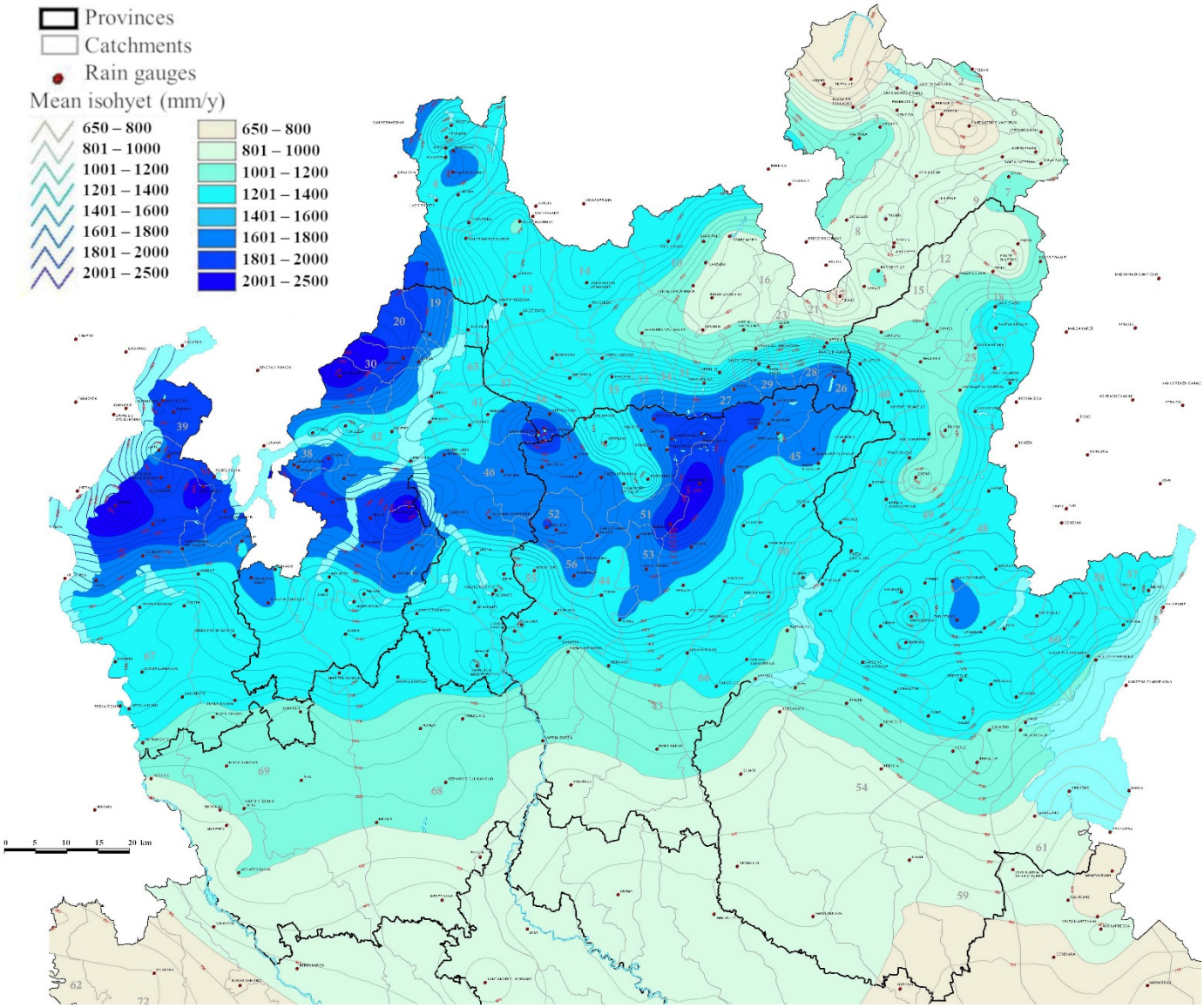

Figure 2. Map of the mean annual precipitation (MAP, in mm/y) in the 1891–1990 period in the alpine and pre-alpine districts of the Lombardy region [84].

2.1.2. Geology and Soils

According to the Italian pedological map system [87], the Alps and Prealps belong to two different soil regions. The alpine region (M1) occupies the northern sectors, with a relief that exceeds 4000 m in elevation along the Swiss border (Bernina Peak, 4049 m a.s.l.); the pre-alpine region (M2) extends through the piedmont and mountain belt enclosed between Lake Maggiore and Lake Garda (Figure 3) and in a small sector in the extreme NE of Lombardy (Figure 3). The two soil regions are differentiated according to the lithological substrate, which is siliceous (igneous or metamorphic) in M1 and sedimentary and carbonatic in M2. This great difference in substrates influences the distribution of soil types. In this work, we associated many soil types in larger groups, mainly characterized by the WRB great groups [88], differentiated according to soil texture, and related with parent material lithology.

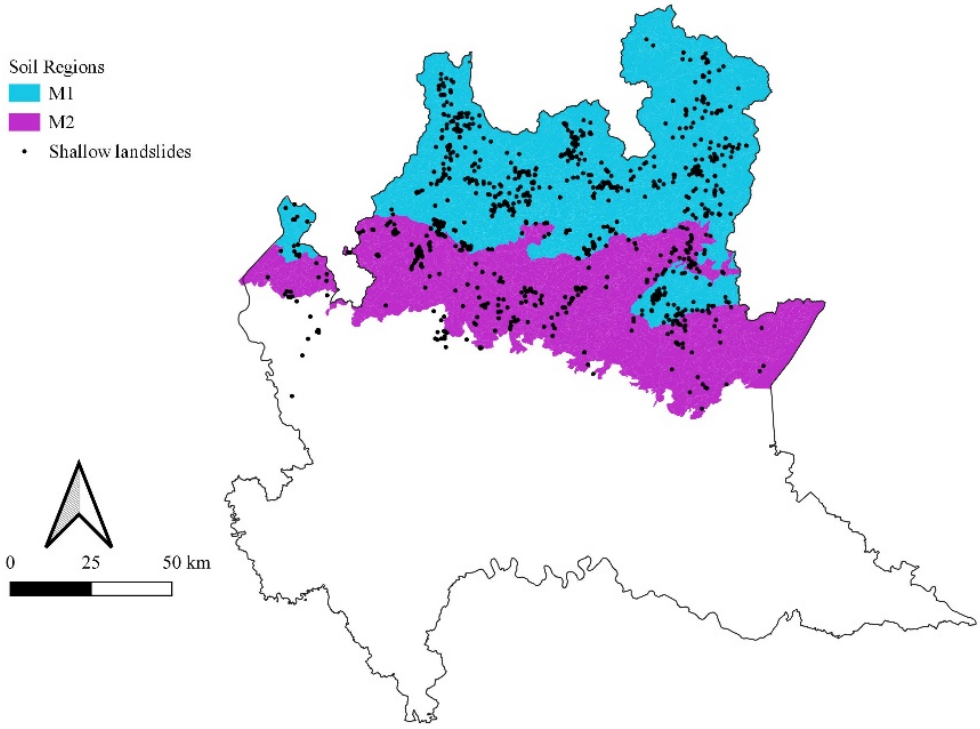

Figure 3. Soil regions included in the study area. Soil regions are based on soil classification by [87]): M1, Central Alps (SR 37.1); M2, Southern Alps (SR 34.3). Black dots represent the shallow landslides and mud-debris flows triggered by rainfall events in the period of 1911–2010, included in the collected database.

According to the soil map of Lombardy (Figure 4) showing the soil typological units (STUs) of the mountain area, Cambisols are the most widespread soils, and they occur on different parent materials, thus showing different properties: in M1, sandy loam Skeletic Cambisols are the most widespread soils, whereas in M2 the Cambisols have a finer (clay loam or loamy) texture. In particular, Leptic and Eutric Cambisols (average depth: 100 cm) are present in approximately 39% of soil region M2, deeper (average depth: 170 cm) clay loam and loamy Leptic and Skeletic Cambisols occur in approximately 15% of the area, and shallower (average depth: 70 cm) clay loamy Leptic and Fluvic Cambisols occur in 7% of the area. Regosols (poorly developed soils) and Leptosols (shallow soils) are common in the Prealps, mainly over limestones and dolostones, and deep Luvisols (developed soils) occur at the boundary with the Po plain. In soil region M1, coarse-textured Umbric and Skeletic Podzols are the second most widespread soil types, whereas sandy loam to loamy sand Humic Umbrisols, with significant topsoil accumulation of organic matter, occur in 19% of the area. Depending on their morphology and position along the slope, their depth ranges from 20 cm to 200 cm. At higher elevations and on the steepest slopes,

shallow soils occur along with eroded soils. Among the former, sandy loam Humic and Skeletic Leptosols occur in 11% of region M1; the latter are mainly Cambic and Leptic Regosols, with an average depth ranging from 25 cm to 60 cm. Fluvisols occur along the bottoms of valleys, are generally characterized by coarse textures (loamy-sand to sandy -loam), and are usually quite thick. In M2, very shallow silty loam to sandy loam Skeletic and Rendzic Leptosols (average depth: 20 cm) occupy approximately 22% of the surface, whereas deep (average depth 180 cm) clay-loam Luvisols are present in the south-eastern margin of the Prealps (6% of the area). Less widespread in soil region M2 are loamy Leptic Phaeozems (shallow, humus-rich soils, average depth 60 cm), deeper silty-loam to sandy loam Umbrisols (average depth: 90 cm), shallower loamy Calcaric and Leptic Regosols, and sandy loam Skeletic Leptosols.

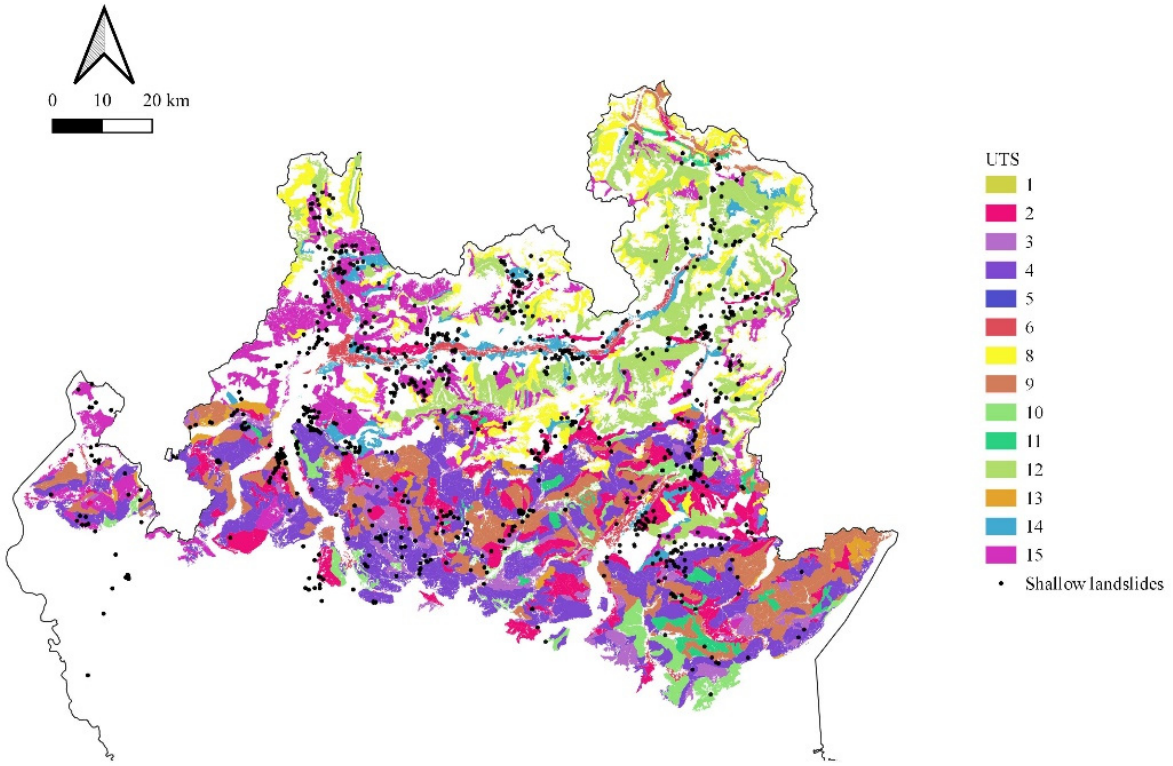

Figure 4. Map of the STU (soil typological unit) of the mountainous area of Lombardy (ref. scale 1:250,000). 1: Skeletic Cambisol; 2: Leptic and Skeletic Cambisol; 3: Leptic and Fluvic Cambisol; 4: Leptic and Eutric Cambisol; 5: Vertic Cambisol and Calcaric Cambisol; 6: Eutric and Haplic Fluvisol; 8: Humic and Skeletic Leptosol; 9: Skeletic and Rendic Leptosol; 10: Luvisol; 11: Leptic Phaeozem; 12: Umbric and Skeletic Podzol; 13: Calcaric and Leptic Regosol; 14: Cambic and Leptic Regosol; 15: Humic Umbrisol. Black dots represent the shallow landslides and mud-debris flows triggered by rainfall events in the period of 1911–2010, included in the collected database.

2.2. Landslides Data Collection

A historical study and analysis of instability processes triggered by rainfall events in Lombardy in the past century was carried out, with particular attention paid to shallow landslides and mud and debris flows that occurred in the Lombard Alps in the period of 1911–2010 (Figure 5). Landslide information was gathered from different sources [89]: (i) the historical archive of CNR-IRPI in Turin, which keeps more than 250,000 unpublished documents on geo-hydrological processes that have occurred in Northern Italy since 1800; (ii) the regional archives of the State Forestry Corps in Milan; (iii) municipal archives; (iv) the Lombardy Geological Survey archive, which has gathered landslide data since the beginning of 19th Century; and (v) scientific papers, technical reports, and newspaper articles (Figure 6).

Figure 5. Example of shallow landslides and mud-debris flows triggered by intense rainfalls in the alpine and pre-alpine provinces of the Lombardy region: (**A**) view of the debris flow that occurred in Vallone di Campo (SO) in 1937; (**B**) view of the soil slips triggered by heavy rainfalls that occurred on 1 June 2002 in Malnate (VA) in the Olona Valley, close to the bridges of the motorway and railway; and (**C**) view of the Rossiga mud-debris flow that occurred in Cortenova (LC) on 27 November 2002. The red arrow indicates the maximum level reached by the debris. (**D**) View of the mud-debris flows that occurred in Brienno (CO) on 7 July 2011 that destroyed some buildings and caused severe damage to structures and infrastructures (image source: CNR-IRPI authors).

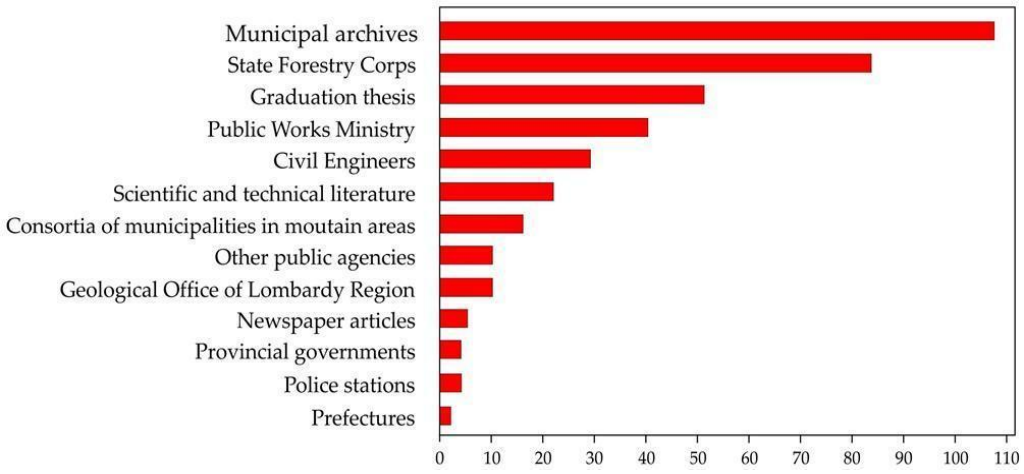

Figure 6. Main sources of mass movement information and correlated number of landslide events.

When the exact position was known, each landslide was georeferenced in a GIS using regional base maps at a 1:10,000 scale and implemented in the catalogue of rainfall-induced shallow landslides and mud-debris flows of the Lombardy region, updating the existing database compiled in [81]. A scheme showing the research steps, data sources, and methods is given in the graphical abstract.

2.3. Rainfall Data Collection

Among the collected data, landslides for which information on the day and time of occurrence was known with sufficient temporal accuracy were considered in further

analyses to associate each individual landslide or group of landslides to the corresponding triggering rainfall event. For this purpose, a spatial analysis was performed to identify the most representative rain gauge. The Lombardy region has a large regional pluviometric database because of a dense network of rain gauges belonging first to the Po Hydrographic Office based in Parma (since 1912), then to the National Hydrographic and Mareographic Service (from 1917), and since 2003, to the Regional Agency for Environmental Protection (ARPA) of Lombardy. The regional hydrological network comprises a total of 318 stations with an average density of one rain gauge every 200 km^2 and it includes both mechanical (the oldest) and automatic systems that operated for different periods. For each landslide, a representative rain gauge was selected within a buffer radius of 5 km centered on the slope failure, considering the irregular spatial distribution of the regional hydrological network and the variability in the rainfall regime due to the morphological setting of the mountain study area. Thunderstorm cells may have occasionally had a limited spatial extent, generating substantial differences in the recorded rainfall amounts between rain gauges in proximity to one another. In the selection of the reference rain gauge, the following criteria were also adopted: (i) minimization of the geographical distance from the landslides, (ii) minimization of the difference in elevation between the rain gauge and the landslide, (iii) location within the same catchment, and (iv) location on a similar slope aspect.

For each reference rain gauge for which hourly rainfall measurements were available, we estimated the rainfall conditions that triggered landslides, e.g., rainfall duration (D, in h), cumulated rainfall (E, in mm), and mean intensity (I, mm/h). As recently proposed in [81] by Luino et al. (2019), a period of at least 12 h with low rainfall intensity (<1 mm/h) was considered for the separation of two rainfall events.

Adopting an approach proposed in the literature [31,81], we also considered the mean annual precipitation (MAP, in mm/y) to consider the influence of the local rainfall regime on the activation of shallow landslides. In particular, for each most representative rain gauge, we obtained the MAP values from the rainfall map proposed in [84] (Figure 4).

2.4. Soil Data Collection

Soil information for the study area was extracted from the pedo-landscape map and database of Lombardy, at a scale of 1:250,000 [90], and from the soil map of Lombardy (1:250,000) [91,92].

The georeferenced soil database at a scale of 1:250,000 covering the whole of Lombardy is also available, including information about soils, organized in four nested levels. From the most general to the most detailed level, 5 soil regions, 18 soil subregions, 65 great soilscapes, and 1038 soilscapes, which are represented by the soil mapping units (SMU) at the 1:250,000 scale, are outlined for the entire region. Each soilscape can include different soil typological units (STU), and any STU can occur in several soilscapes. The STUs were classified according to the World Reference Base for Soil Resources (WRB) [88]. The map shown in Figure 4 shows the dominant STU identified for each SMU of the alpine and pre-alpine area of Lombardy.

For each shallow landslide site in the study area, the following information for the respective SMUs were extracted from the available maps and databases: the soil region of each soilscape; the WRB classification of each STU at the subunit level, grouped by texture and thickness class; the surface stoniness (%) and rockiness (%); the soil depth (cm); the USDA textural class, up to 1 m deep; the skeleton content, up to 1 m deep (%); and the organic carbon content, up to 1 m deep (%).

The digital terrain model (DTM) (20 m resolution) and CORINE Land Cover (1990 and 2000) data for the study area were also obtained from the "Geoportale della Lombardia" (https://www.geoportale.regione.lombardia.it/, Last accessed: 13 December 2021). The average elevation (m) and slope (%) were calculated for each landslide site based on the 20 m DTM and by adopting a buffer with a radius of 40 m centered on the landslide location.

2.5. Database Creation

Based on the abovementioned data on landslides that occurred in the study area, associated precipitation and soil properties, a database including all or part of the following information for each rainfall-triggered landslide (N = 1035) was created, including:

(1) Landslide occurrence and type: date and season of occurrence, SS (soil slip) or MDF (mud and debris flow).
(2) Location and topographical information: coordinates, municipality, province, catchment, elevation (min, max, and average), and slope (min, max, and average).
(3) Land use.
(4) Geological and pedological information: lithology, soil region, soil province, dominant STU, WRB classification; for the first meter of soil: stoniness, rockiness, depth, texture, skeleton, and organic carbon content.
(5) Rainfall characteristics: MAP; triggering rainfall characteristics: cumulated precipitation, duration, and hourly intensity.

2.6. Statistical Analysis

To investigate the role of rainfall in local soil and landscape processes, ANOVA ($p < 0.05$) was conducted to compare the rainfall characteristics triggering landslides in different soil contexts. The Pearson correlation matrix ($p < 0.05$) was used to highlight the relationships among soil properties (stoniness, rockiness, depth, skeleton, and organic carbon content), topographical (elevation and slope), and precipitation variables (duration, cumulated precipitation, and intensity) associated with triggered landslides.

2.7. Definition of Rainfall Thresholds

In the literature, most of the methods proposed to define rainfall thresholds lack explanations of the mathematical or statistical criteria adopted, meaning that they are very frequently not objective and difficult to reproduce [26,27].

In this study, we adopted the frequentist approach proposed in [89] by Brunetti et al. (2010) to define an intensity–duration (ID) rainfall threshold curve for the possible initiation of shallow landslides, based on the simple power law:

$$I = \alpha D - \beta, \quad (1)$$

where I is the mean rainfall intensity (in mm/h), D is the duration of the rainfall event (in h), α is a scaling constant which represents the intercept of the curve, and β is the shape parameter that defines the slope of the curve. The frequentist method relies on a frequency analysis of the rainfall conditions that resulted in the observed landslides. Based on the distribution of observed empirical data, this approach is sensitive to data dispersion. First, we log-transformed the empirical rainfall intensity and duration data and fitted them with a linear equation of the type $\log(I) = \log(\alpha) - \beta \log(D)$, using the least-squares method. For each rainfall event, we calculated the difference $\delta(D)$ between the logarithm of the event intensity, log[I(D)], and the related intensity value of the fit log, log[If(D)]. Next, we estimated the probability density function (PDF) of the distribution of the differences $\delta(D)$ between the event intensity and the corresponding values estimated with the least-squares fit. The PDF of the distribution of $\delta(D)$ was calculated using the kernel density estimation, a non-parametric technique that considers the noise of observed data [93–95]. Kernel density estimation can produce misleading results, particularly for small data sets, if the kernel width, h, is poorly chosen. When this smoothing parameter is too small, the final curve may exhibit undue fine structures; when it is too large, the final curve may depart from normality. Thus, an optimal value of the kernel width must be carefully chosen. Following the recommendation of Silverman [94], a default width of 0.9*min (s, IQ/1.34) $n - 0.2$ has been adopted, where s is the sample standard deviation and IQ is the interquartile range of the sample population. The resulting PDF was then fitted with a Gaussian function adopting the least-squares method. The frequentist approach

allows one to define a number N of thresholds corresponding to N probability levels of exceedance. This means that different acceptable numbers of triggered landslides can be defined when adopting thresholds for warning purposes. In the present work, we selected the threshold probability level of 5% and 10% for the pedological and regional thresholds, respectively, corresponding to the threshold that leaves 95% and 90% of the empirical points above the fitting curve in the correlated diagrams.

Finally, we defined the ID thresholds for any given probability of exceedance based on the modeled fitted distribution of δ(D), both for all the rainfall events and for the events falling in each pedological domain, obtaining 9 thresholds: (i) 1 regional threshold for the entire Lombardy Alps and Prealps (subSection 3.3); (ii) 2 thresholds for soil region: M1 and M2 (subSection 3.4.1); (iii) 2 thresholds for different soil texture: coarse textured soils and fine textured soils (subSection 3.4.2); and (iv) 4 thresholds for soil groups: Cambisol coarse and skeletal soils, Cambisol fine soils, Podzol soils, and Umbrisol soils (subSection 3.4.3).

Furthermore, using the subset of landslides that occurred in the Varese, Como, Lecco, and Bergamo Provinces, new regional thresholds (subSection 3.3) were derived for shallow landslides and mud-debris flows in the corresponding alpine and pre-alpine districts of the Lombardy region. For this purpose, we estimated the MAP-normalized mean rainfall intensity (IMAP, in h^{-1}) and the % MAP-normalized mean rainfall intensity (IN, as a percentage), according to the approach recently applied for the Valtellina and Valcamonica valleys in [81].

3. Results

3.1. Soil Properties and Landslide Occurrence

The database obtained through the survey of the various sources included 1035 landslides. Some of them were located in areas for which the soil characteristics are not fully known according to the available soil map. The number of failures that could be attributed to a specific SMU with complete information was 891 (86% of the total). For each STU in identified in the study area, Table 1 shows the extension (in km^2 and as a percentage), the classification of the dominant soil(s), the average depth of the soil profile and its textural class(es), and the number of recorded landslides and the landslide density. The occurrence of failures was different in the various STUs. The textural class was known for each STU, so this parameter could be used as an additional criterion to guide the definition of the soil-specific thresholds. STUs with a coarser texture (SL or LS), mostly located on siliceous substrates in M1, had a relatively higher number of failures (66% of the total recorded events) with a density of 0.14 landslides/km^2, which was almost twice the density observed in the finer-textured units (0.08 landslides/km^2), which mostly developed in M2. Coarse-textured Skeletic Cambisols (Sandy-loam or Loamy-sand) showed the highest landslide density in both soil regions, with 0.23 and 0.34 failures/km^2 in M1 and M2, respectively. The "Skeletic Cambisols" in M2 were outliers in the M2 region, likely formed on glacial till. Apart from the STUs defined by organic matter-rich soils, such as Umbrisols and Podzols, the units with deeper soils were characterized by a higher density of failures.

Table 1. Extension (in km^2 and as a percentage), classification of the dominant soil(s), average depth of the soil profile and its textural class(es), number of recorded landslides, and landslide density for each soil typological unit (STU) identified within the soil regions M1 and M2 of the Alps and Prealps of Lombardy. SL: Sandy Loam; LS: Loamy Sand; L: Loamy; CL: Clay-loam; SiL: Silt Loam; SCL: Silty Clay Loam.

Soil Region	STU ID	Area km^2	% Area/Region	Dominant Soils	Average Depth, cm	Textural Class	N° of Landslides	Landslide Density (N/km^2)
M1	1	1365	34%	*Skeletic Cambisol*	150	SL	309	0.23
M1	12	932	23%	*Umbric* and *Skeletic Podzol*	150	SL	65	0.07
M1	15	766	19%	*Humic Umbrisol*	90	SL (LS)	99	0.13
M1	8	456	11%	*Humic* and *Skeletic Leptosol*	30	SL (L)	13	0.03
M1	14	225	6%	*Cambic* and *Leptic Regosol*	60	SL-LS	34	0.15

Table 1. *Cont.*

Soil Region	STU ID	Area km^2	% Area/Region	Dominant Soils	Average Depth, cm	Textural Class	N° of Landslides	Landslide Density (N/km^2)
M1	2	160	4%	*Skeletic Cambisol*	200	SL (LS)	54	0.34
M1	6	111	3%	*Eutric Fluvisol*	120	SL	-	-
M1	0	17	0%	*Skeletic Fluvisol* and *Leptic Regosol*	25	SL-LS	-	-
M2	4	1491	39%	*Leptic* and *Eutric Cambisol*	100	CL e L	114	0.08
M2	9	858	22%	*Skeletic* and *Rendzic Leptosol*	20	L-SL (SiL)	45	0.05
M2	2	570	15%	*Leptic* and *Skeletic Cambisol*	170	L (CL)	85	0.15
M2	3	274	7%	*Leptic* and *Fluvic Cambisol*	70	CL	15	0.05
M2	10	231	6%	*Luvisol*	180	CL (SCL)	33	0.14
M2	11	130	3%	*Leptic Phaeozem*	60	L (SL)	8	0.06
M2	15	124	3%	*Umbrisol*	90	SL (SiL)	11	0.09
M2	13	94	2%	*Calcaric* and *Leptic Regosol*	60	L (CL)	5	0.05
M2	8	57	1%	*Skeletic Leptosol*	40	SL	1	0.02
M2	6	21	1%	*Haplic Fluvisol*	150	SL	-	-

More detailed information was available for the first meter of soil of each STU. Table 2 shows the descriptive statistics of the soil depth, the surface stoniness and rockiness, and the skeleton and organic carbon contents of the study area and of each soil region within it (M1 and M2). Soils of region M1 were characterized by a significantly ($p < 0.05$) higher surface stoniness, rockiness, skeleton, and organic carbon content and a lower soil depth than region M2. Both the average elevation and slope of the landslide sites were significantly higher for landslides that occurred in M1 than those occurred in M2.

Table 2. Descriptive statistics of the available soil information that referred to the delineation of the soil map at the scale of 1:250,000 and presented for the whole study area and for the M1 and M2 soil regions. Different letters indicate significant differences according to ANOVA ($p < 0.05$). * Topographic variables (elevation and slope) were obtained from DTM for triggered landslides for which exact localization was known (N = 872). Different letters indicate significant differences according to ANOVA ($p < 0.05$).

	Num	Mean	St. Dev	Min	Median	Max
Surface Stoniness (%)	10,987	12.19	13.53	0.00	6.00	80.00
M1	5621	14.86 a	12.54	0.00	16.00	35.00
M2	4868	10.10 b	14.44	0.00	1.00	80.00
Surface Rockiness (%)	10,987	10.36	9.00	0.00	10.00	65.00
M1	5621	12.55 a	9.34	0.00	12.00	65.00
M2	4868	8.89 b	7.97	0.00	5.00	32.00
Depth (cm)	10,987	93.02	71.86	8.00	73.00	294.00
M1	5621	86.57 a	61.78	8.00	73.00	204.00
M2	4868	96.91 b	80.36	11.00	55.00	294.00
Skeleton, up to 1 m depth (%)	10,987	30.81	16.70	0.00	32.00	80.00
M1	5621	35.98 a	10.61	3.00	35.00	69.00
M2	4868	27.15 b	19.75	4.00	21.00	80.00
Organic C, up to 1 m depth (%)	10,987	2.99	2.17	0.70	2.20	11.10
M1	5621	3.56 a	2.11	0.80	2.40	8.50
M2	4868	2.29 b	1.66	0.70	1.90	9.50
Elevation *, average (m a.s.l.)	872	912.7	484.4	211.6	822.6	2453.3
M1	564	1044.1 a	456.4	242.1	981.2	2453.3
M2	318	683.8 b	324.2	211.6	642.7	2012.5
Slope *, average (%)	872	58.30	23.77	3.72	56.46	141.47
M1	554	62.12 a	20.83	3.72	61.02	141.47
M2	318	51.63 b	22.77	4.86	49.79	141.00

3.2. Relationships among Soil and Rainfall Characteristics for Events Triggering Landslides

For the 357 landslides included in the database, the rainfall event that likely triggered each one was determined and characterized in terms of the rainfall duration and intensity. Table 3 summarizes the descriptive statistics for the rainfall events for the entire study area and for the two soil regions, M1 and M2. The rainfall events that resulted in landslides in the two soil regions were characterized by significantly different mean durations and intensities ($p < 0.05$). In soil region M1, the triggering rainfall events were longer-lasting and less intense than those in M2; in particular, they had a mean duration of 33.5 h, whereas in M2 the mean duration of the rainfall events was about 27 h. The observed mean hourly intensity in soil region M2 (8.2 mm/h) was nearly double the mean hourly intensity observed in soil region M1 (4.6 mm/h). The average triggering cumulative rainfall was lower in soil region M1 (96 mm) than that recorded in soil region M2 (108 mm); however, in this case, the difference between the two means was not significant. The Pearson correlation matrix among the soil, topographical, and precipitation characteristics of the triggered landslides (Table 4) showed that, among the available soil characteristics, the soil depth correlated most with the characteristics of the rainfall events resulting in landslides. Soil depth was negatively correlated with rainfall intensity ($r = -0.23$) and positively correlated with rainfall duration ($r = 0.16$); both correlations were significant at $p < 0.05$. Thus, the rainfall events resulting in slope failures were longer when the soil was deeper, whereas the opposite relationship was observed with rainfall intensity; indeed, short events of high intensity appeared to be more likely to trigger landslides in shallow soils. The organic carbon content and rock fragment percentages were not significantly correlated with the characteristics of rainfall events that triggered landslides, whereas the percentage of stones at the soil surface was significantly and negatively correlated with rainfall intensity ($r = -0.16$). The correlations between the elevation and slope around the locations of landslides versus the rainfall characteristics were not statistically significant. On the contrary, significant and positive correlations existed between the topographical characteristics (elevation and slope steepness) and stoniness and rockiness. In addition, the steepest slopes, in places where landslides were triggered, also had the shallowest soils.

Table 3. Descriptive statistics of the rainfall events triggering landslides in the two soil regions (M1 and M2) and in the entire study area. Mean values followed by different letters are significantly different at the $p < 0.05$ level, according to ANOVA test.

	Mean	Number of Events	Std. Dev.	Minimum	Median	Maximum
Cumulative Precipitation, mm						
Soil region M1	95.6 a	246	72.7	6.3	80.8	382.0
Soil region M2	107.9 a	111	79.8	2.0	79.5	382.0
All events	99.4	357	75.1	2.0	80.0	382.0
Duration, h						
Soil region M1	33.5 a	246	27.1	1.0	32.0	110.0
Soil region M2	27.1 b	111	26.1	1.0	19.0	106.0
All events	31.4	357	26.0	1.0	28.0	110.0
Intensity, mm/h						
Soil region M1	4.6 a	246	4.7	0.3	2.9	31.8
Soil region M2	8.2 b	111	9.4	1.0	4.5	39.0
All events	5.7	357	6.7	0.3	3.1	39.0

Table 4. Correlation matrix between soil and rainfall variables associated with landslides (N = 297); in bold; statistically significant values ($p < 0.05$). Ston.: surface stoniness (%); Rock.: surface rockiness (%); Depth: soil depth (cm); Skel.: skeleton (%); C org.: soil organic carbon (%); D: rainfall duration (h); Pc: cumulative precipitation (mm); I: rainfall intensity (mm/h); EL: elevation from digital elevation model, mean value within a buffer of 40 m radius centered on landslide location (m a.s.l.); SLP: slope from digital elevation model, mean value within a buffer of 40 m radius centered on landslide location (%).

	Ston.	**Rock.**	**Depth**	**Skel.**	**C org.**	**D**	**Pc**	**I**	**EL**	**SLP**
Ston.	1	0.11	0.10	0.18	0.12	0.04	−0.04	−0.16	0.25	0.12
Rock.		1	−0.53	0.21	0.49	0.01	−0.02	−0.07	0.12	0.22
Depth			1	−0.14	−0.46	0.16	0.04	−0.23	−0.07	−0.18
Skel.				1	0.17	0.01	−0.07	−0.02	0.33	0.10
C org.					1	−0.09	−0.10	−0.02	0.28	0.02
D						1	0.78	−0.47	−0.05	−0.01
Pc							1	−0.12	−0.11	0.02
I								1	−0.03	−0.01
EL									1	0.13
SLP										1

3.3. Regional Thresholds

Based on the information collected in the study about rainfall induced landslides in the period 1911–2010, three regional thresholds were defined, disregarding soil characteristics. The first ID threshold was defined using the frequentist approach for the Lombard Alps and Prealps:

$$I = 7.138\ D^{-0.442} \quad (2)$$

based on the dataset including 343 landslides (out of 357) for which rainfall and soil data were fully known. The excluded landslides lacked rainfall information suitable to define the thresholds. Two regional thresholds (for different rainfall durations) were obtained using a subset of 86 events that occurred in the Varese, Como, Lecco, and Bergamo Provinces, to identify the rainfall conditions that were likely to initiate shallow landslides and mud-debris flows in this alpine and pre-alpine sector of the Lombardy region. According to [81], we divided spring-autumn and summer events to consider their differences in rainfall conditions that resulted in landslides. We noted that the empirical I_N-D points representative of spring-autumn events largely converged on duration values higher than 10 h and MAP-normalized intensity values ranging from 0.1% and 0.4%, whereas points representative of summer events were dispersed, including both short and very heavy rainfalls or thunderstorms and prolonged precipitation events with a duration D > 10 h. Consequently, the rainfall conditions responsible for the landslide activation were analyzed separately for each range of duration. Figure 7 shows the I_N-D thresholds calculated at a 10% exceedance of the probability level in the relative ranges of duration:

$$I_N = 0.57\ D^{-0.43}\ D \leq 10\ h, \quad (3)$$

$$I_N = 0.33\ D^{-0.19}\ D > 10\ h \quad (4)$$

The parameters defining the thresholds are shown in Table 5, which can be compared to other thresholds obtained for specific soil conditions and with reference thresholds already available for the study area.

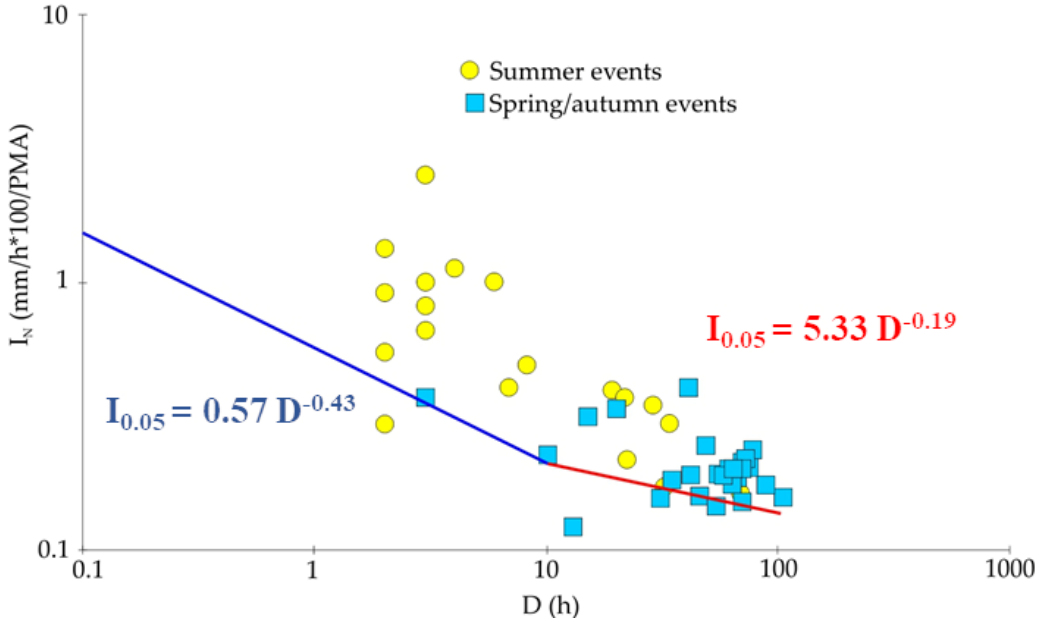

Figure 7. Rainfall events (colored marks) that resulted in soil slips and mud-debris flows in the Varese, Como, Lecco, and Bergamo Provinces in the period of 1911–2010. Colored lines represent thresholds that leave 90% empirical points I_N-D above the curve for different ranges of duration (blue, < 10 h; red, > 10 h).

Table 5. New regional and pedological ID thresholds defined in this work and similar ID thresholds derived from the literature for the same area. Delta is the uncertainty for the parameters α and β of the threshold curves; D represents the rainfall duration (in h).

	Events	Intercept, α	Slope, β	Delta α	Delta β	D Range
New thresholds						
Regional thresholds						
Lombardy Alps and Prealps (Equation (2))	343	7.138	−0.442	0.854	0.022	1 < D < 110
Varese, Como, Lecco, and Bergamo (Equation (3))	86	0.57	−0.43			0.2 < D < 10
Varese, Como, Lecco, and Bergamo (Equation (4))	86	0.33	−0.19			10 < D < 100
Soil region thresholds						
Soil region M1 (Equation (5))	241	3.330	−0.379	0.522	0.024	1 < D < 110
Soil region M2 (Equation (6))	102	18.465	−0.532	1.184	0.038	1 < D < 106
Soil texture thresholds						
Coarse textured soils (Equation (7))	206	4.985	−0.408	0.608	0.029	1 < D < 110
Fine textured soils (Equation (8))	89	18.019	−0.528	1.050	0.039	1 < D < 106
Soil group thresholds						
Cambisol coarse and skeletal soils (Equation (9))	107	5.087	−0.393	0.706	0.038	1 < D < 110
Cambisol fine soils (Equation (10))	68	17.141	−0.534	1.234	0.049	1 < D < 106
Umbrisol soils (Equation (11))	36	8.225	−0.437	0.915	0.074	2 < D < 67
Podzol soils (Equation (12))	27	8.868	−0.426	0.939	0.070	1 < D < 70
Reference thresholds						
Sondrio and Brescia (Luino et al., 2019) [43]	291	0.58	−0.46			0.2 < D < 10
Sondrio and Brescia (Luino et al., 2019) [43]	291	0.31	−0.19			10 < D < 100
Lombardia (Ceriani et al., 1994) [96]	-	20.10	−0.550	-	-	1 < D < 1000
Valtellina (Cancelli and Nova, 1985) [97]	-	44.67	−0.780	-	-	1 < D < 1000

3.4. Soil-Based Rainfall Thresholds

Given the different types of information included in the database, several possible criteria were tested to define the soil-based rainfall thresholds for landslide initiation in the Alps and Prealps of Lombardy. Three groups of rainfall thresholds were defined based on the soil regions, soil textures, and soil types, using different subsets of the 343 landslides, corresponding to the events that took place in each separated domain.

The results are summarized in Table 5, which shows the number of observations used to define each threshold, the two parameters defining the curve along with their 95% confidence intervals, and the range of applications in terms of rainfall duration. In all cases, the threshold probability level selected was equal to 5%.

3.4.1. Thresholds Defined by Soil Region

The first type of threshold was defined by distinguishing the two soil regions (M1 and M2). The two curves were clearly distinguishable and did not overlap; in addition, no overlapping was observed for the limit curves defining their 95% confidence limits (Figure 8). The ID threshold curve for soil region M1 (Equation (5), N = 241) had an intercept α and a slope β equal to 3.330 ($\pm$0.522) and $-$0.379 ($\pm$0.024), respectively. The corresponding values for α and β of the 5% ID threshold curve for soil region M2 (Equation (6), N = 102) were 18.465 ($\pm$1.184) and $-$0.532 ($\pm$0.038), respectively, resulting in a difference between the two thresholds that is large and statistically significant ($p < 0.05$), as their 95% confidence intervals did not overlap for rainfall durations between 1 and 110 h. For the sake of comparison, the 5% ID threshold curve for the entire Lombardy Alps and Prealps study area (Equation (2), N = 343) was also reported (blue curve in Figure 8), and their intercept α and slope β were equal to 7.138 ($\pm$0.854) and $-$0.442 ($\pm$0.022), respectively.

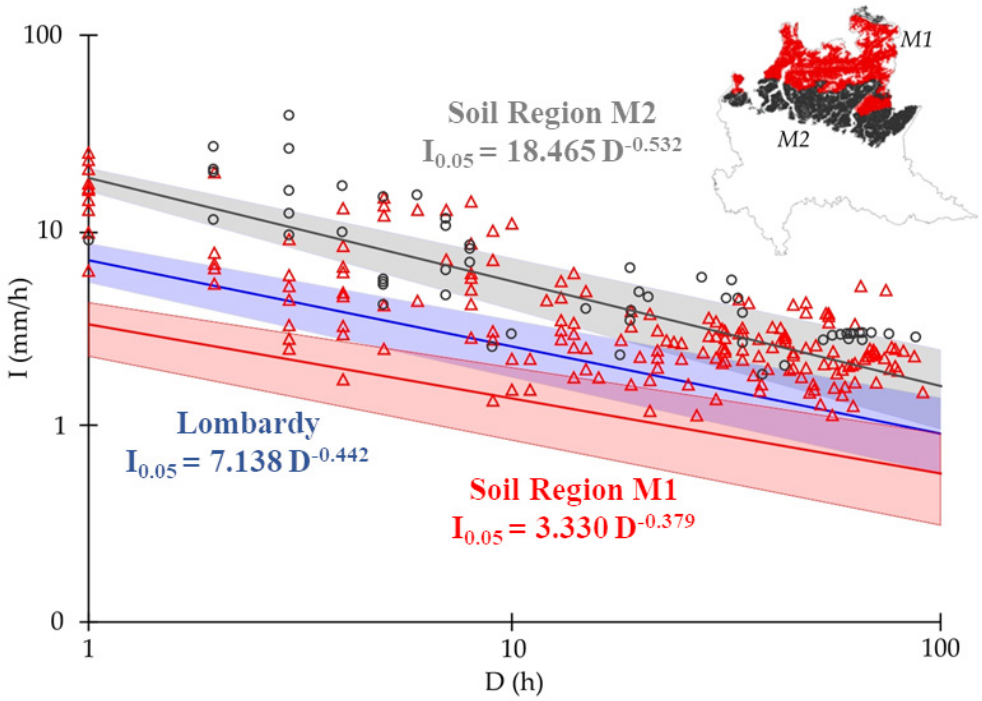

Figure 8. Rainfall intensity–rainfall duration (ID) thresholds for the whole data set and for the two soil regions (M1 and M2) (see Table 5. Colored lines are 5% power law thresholds. Shaded areas between dashed lines show 95% confidence intervals of the threshold curves.

3.4.2. Threshold Defined by Soil Texture

A second criterion that allows for the definition of soil-based rainfall thresholds is based on soil texture. Thus, to define rainfall thresholds based on soil texture, textural classes were grouped into the two following textural families: fine (N = 89), including the clay, clay loam, silt loam, and loam textural classes, and coarse (N = 206), including the sandy loam and loamy sand textural classes. The corresponding 5% ID threshold curves are shown in Figure 9, along with their 95% confidence intervals. The curves are clearly identifiable, but the confidence intervals overlap for D > 35 h. The 5% ID threshold curve for the coarse-textured soils (Equation (7), N = 206) had an intercept α and slope β equal to 4.985 ($\pm$0.61) and $-$0.408 ($\pm$0.03), respectively. The corresponding values for α and

β of the 5% ID threshold curve for the loam to fine textured soils (Equation (8), N =102) were 18.019 (±1.050) and −0.528 (±0.039), respectively. The difference between the two thresholds was large and statistically significant ($p < 0.05$) and this clearly highlights the greater susceptibility to slope failure that is characterized by coarse-textured soils. For these soils, the duration and the amount of rainfall that could result in a landslide were significantly smaller than those necessary to trigger slope failures on loam to fine-textured soils (in the range of rainfall durations between 1 and 106 h).

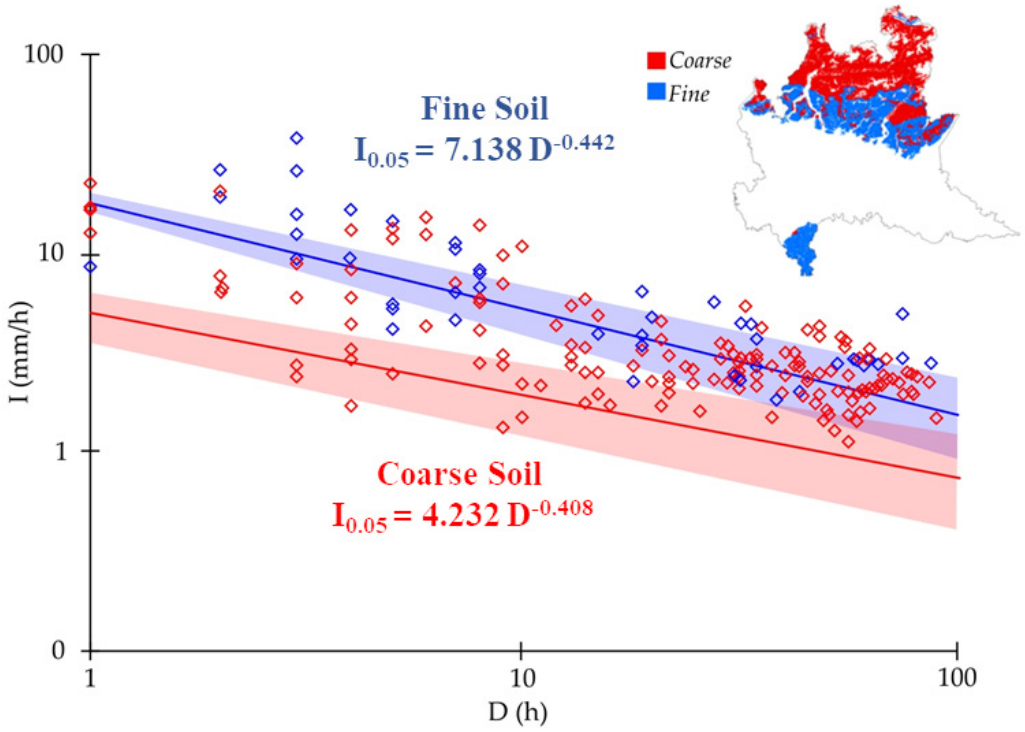

Figure 9. Rainfall intensity–rainfall duration (ID) thresholds for fine- and coarse-textured soils (see Table 5). Colored lines are 5% power law thresholds. Shaded areas between dashed lines show the 95% confidence intervals of the threshold curves.

3.4.3. Threshold Defined by Soil Groups

To further explore and elucidate the possible role of soil properties in responding to rainfall events, an additional grouping criterion based on the main soil formation processes and soil texture was considered. For this analysis, the landslides were divided into and considered in four groups representing the well-defined soil types where they occurred: (i) coarse and skeletal Cambisols (Equation (9), N = 107; STU 1 in Figure 3), mostly falling in soil region M1; (ii) fine Cambisols (Equation (10), N = 68; STU 2, 3, and 4 in Figure 3), mostly falling in soil region M2; (iii) Umbrisols (Equation (11), N = 36; STU 15), mostly falling in soil region M1; and (iv) Podzols (Equation (12), N = 27, STU 12 in Figure 3) falling entirely in soil region M1. These last two groups, although very different in terms of their dominant soil forming processes, were characterized by a dominant sandy loamy texture and organic matter accumulation. The different 5% ID threshold curves are shown in Figure 10, along with their 95% confidence intervals; their parameters, intercept α and slope β, are shown in Table 5, along with their errors. The four curves did not intersect for $1 < D < 110$. The difference among the curves was statistically significant ($p < 0.05$) between the two groups of Cambisols for $D < 13$ h, and among the Umbrisols and Podzols and the fine Cambisols for $D < 2.5$ h. They were almost parallel, on a log-log plot, with an intercept α, which was minimal for the coarse and skeletal Cambisols (α = 5.087 ± 0.706) and maximal for the fine Cambisols (α = 17.141 ± 1.234). The values of α for Umbrisols and Podzols were similar—equal to 8.225 ± 0.915 and 8.868 ± 0.939, respectively. The slope of the curve was slightly steeper for the fine-textured Cambisols

($\beta = -0.534 \pm 0.49$) than for the coarse-textured Cambisols ($\beta = -0.393 \pm 0.038$); again, the values for Umbrisols and Podzols were very similar—equal to -0.437 ± 0.074 and -0.426 ± 0.070, respectively. It must be noted that Umbrisols, Podzols, and coarse and skeletal Cambisols mostly occurred in the same soil region M1; the differences observed in their rainfall threshold curves, given the similar textural composition, are likely explained in terms of the organic matter content in the soil profile through its effects on the soil structure and hydraulic properties. Given the same rainfall duration $1 < D < 110$, the cumulative rainfall Pc corresponding to a given intensity I increased according to the following order: coarse and skeletal Cambisols < Umbrisols ≤ Podzols < Fine Cambisols.

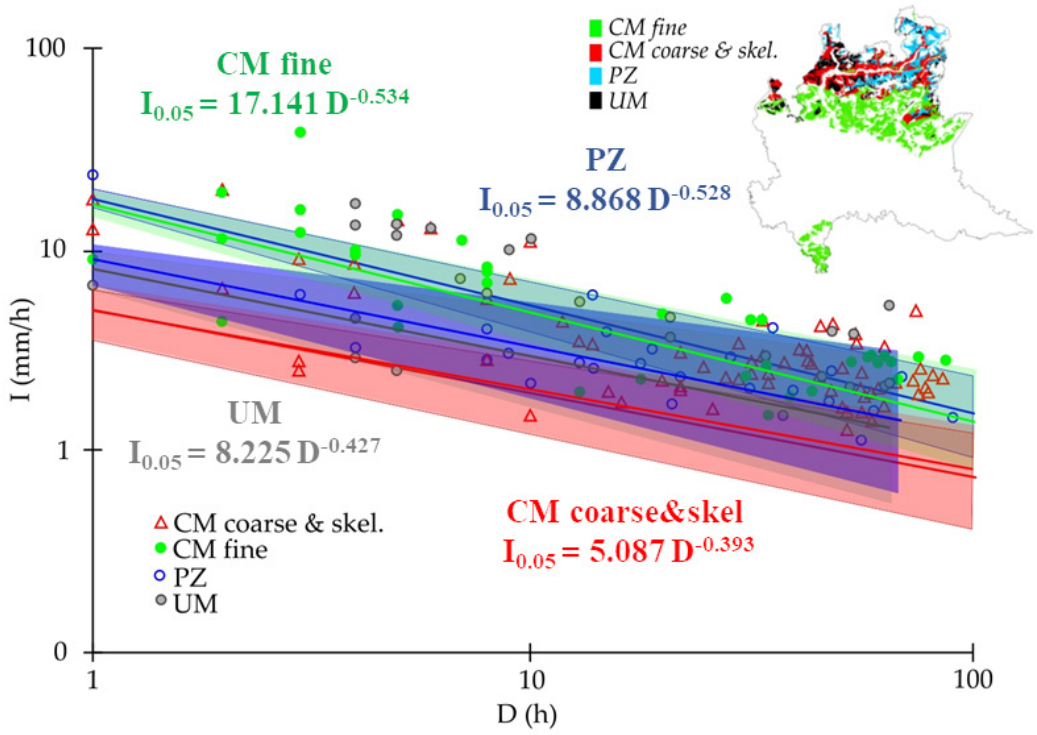

Figure 10. Rainfall intensity–rainfall duration (ID) thresholds for four different soil types: Cambisols fine soils (CM fine); Cambisols coarse and skeletal soils (CM coarse & skel.); Podzol soils (PZ); Umbrisol soils (UM). Colored lines are 5% power law thresholds. Shaded areas between dashed lines show the 95% confidence intervals of the threshold curves.

4. Discussion

According to the results of the study carried out by Luino et al. [65] in the Valtellina and Valcamonica areas (Sondrio and Brescia Provinces), the analysis of the rainfall-induced shallow landslides observed in the rest of the alpine and pre-alpine territory within Lombardy (Varese, Como, Lecco, and Bergamo Provinces) in the period of 1911–2010 highlighted a seasonal variability in the rainfall conditions that triggered slope failures. Spring and autumn events were usually associated with long-lasting ($D > 10$ h) but moderate- or low-intensity ($0.1\% < IN < 0.4\%$) precipitations. Summer events showed substantial differences in rainfall durations, including both high-intensity and short-duration thunderstorms and prolonged precipitations ($D > 10$ h). The variability in the rainfall conditions is correlated with the differentiated mechanical responses of soil to hydrological loading in terms of stability. Spring and autumn slope failures are usually prompted by the deep and complete saturation of the materials in the period that precedes the paroxysmal phase, favored by prolonged precipitations. On the contrary, short and very intense rainfalls or thunderstorms typical of summer months quickly cause the saturation of the shallow layers of soil, impeding further infiltration processes down in the deeper soil levels. Moreover, the established curve shows different slopes in the range of duration; it is steeper for short-duration ($\beta = 0.46$

for D < 10 h) than for long-duration ones (β = 0.19 for D > 10 h). This highlights that the initiation of rainfall-induced shallow landslides is closely correlated with the rainfall duration when the failures are activated by short and intense precipitation, rather than in cases of prolonged and moderate events.

Table 5 summarizes the comparison between the new pedological thresholds established using all the events falling within the Alps and Prealps of the Lombardy region and those falling within each separate homogeneous domain, and the new regional rainfall threshold obtained for the Varese, Como, Lecco, and Bergamo Provinces, along with other similar curves proposed in the literature for the same territory: (i) the regional threshold defined in [81] by Luino et al. for the Sondrio and Brescia Provinces, (ii) the regional curve obtained in [97] for the Valtellina Valley, and (iii) the regional threshold proposed in [96] for the entire Lombardy region.

The regional curves for the alpine and pre-alpine provinces were very similar. As shown in Table 5, the intercept α and slope values β of the new threshold for the Varese, Como, Lecco, and Bergamo Provinces and those obtained in [81] for the Sondrio and Brescia Provinces are comparable in their ranges of duration. We attribute this close correlation to the similar approach adopted in collecting and elaborating the rainfall and landslide information and in defining the thresholds.

However, the new regional threshold was lower to significantly lower than the regional curve proposed in [88] for the entire Lombardy region and the one defined in [97] for the Valtellina Valley. In particular, for a rainfall period with a small duration (D < 10 h), the new curves proposed in this work are lower than the previous regional thresholds; for a rainfall period with a long duration (D > 10 h), the comparison reveals a gradual convergence between the curves, in particular for rainfall durations exceeding 50 h. Moreover, we noted that the new curves established for the Varese, Como, Lecco, and Bergamo Provinces were gentler (β = 0.19) than those obtained for the Lombardy region (β = 0.55) and Valtellina (β = 0.78). We attribute this result firstly to the different landslide and precipitation information and the different approach adopted in defining the rainfall thresholds. According to the method of Luino et al. (2019), we can explain the low curve obtained in the present work by adopting more precautionary critical rainfall conditions than those previously defined. Regardless of the soil-based criteria used to group the available observations, the results obtained in this study suggest that the shallow landslides in the study area are triggered by rainfall events of smaller intensities and shorter durations than those which were previously believed [96,97].

The most widespread soils in the study area are Cambisols, which are fairly developed soils and that represent the third most prevalent type of soil in Europe [98]. Among them, in particular, Skeletic Cambisols showed the highest landslide density in both the M1 and M2 regions. These soils were characterized by a high percentage of rock fragments (>40%) and SL/LS textural classes, which resulted in lower rainfall triggering thresholds compared to finer soils, both considering the thresholds defined considering the soil region and considering the soil texture. Similarly, in a study on rainfall-induced landslides in Central Nepal, Eutric Cambisols showed a strong association with the occurrence of landslides [99].

Within the study area, soils that developed over calcareous parent materials were prevalent in Southern Alps (M2), characterized by a deeper profile and a finer texture. They had a rainfall threshold persistently higher than the threshold established for soils developed over siliceous parent materials with a coarser texture and a shallower depth, typical of the Central Alps sector (M1). In M1, landslides occurred at higher elevations and on steeper soils than in M2, where soils are usually characterized for greater stoniness and rockiness in the first meter and lower average soil depth than in the soil region M2. Dapporto et al. [100] analyzed shallow failures that occurred in the Albaredo valley, which was triggered by the event of 14–16 November 2002 on 1.1 m thick colluvial soil (silty sand, horizons A and B) overlaying a 1 m thick coarse glacial deposit (horizon C) and the bedrock (D). The authors conducted an analysis of slope instability, based on the mechanical and hydraulic properties of soils derived from experimental data and from the literature. Their

results showed that a positive pore pressure was recorded after 15 November, originating in the lower horizon (C), and progressively increasing in thickness, with a temporary saturated zone developing and reaching the surface. The Albaredo Valley's landslides were included in the database compiled in our study, with triggering rainfall having a duration D of 55 h and a rainfall intensity I of 3.83 mm/h. The landslide's location was included in soil region M1, with loamy sand, and then coarse soil. Indeed, the landslides occurred above all the thresholds defined in this study, close to the upper 95% confidence interval for the fine soils and fine Cambisols. With respect to the coarse soil thresholds, the point representing the triggering rainfall condition is clearly above the threshold, thus indicating that the triggering conditions could be correctly identified. The stability of a slope, especially when it is potentially subject to rainfall-induced shallow landslides, strongly depends on the soil's water content. The results match expectations based on the assumption that given the same soil moisture conditions prior to the triggering event, the total critical amount of rainfall required to saturate a uniform soil slope to a critical depth depends on the soil retention properties [101,102]. Given some simplified assumptions, such as the total infiltration of the rainfall, the total critical amount of rainfall (Rc) necessary to saturate the soil to a critical depth (Dc) and cause a slope failure is proportional to the difference between the water content at saturation (θs) and the water content at field capacity (θf) [103]. In the case of fine-textured soil, the difference between the water content at saturation and the water content at field capacity is normally higher than in coarse-textured soils. Consequently, the total critical amount of rainfall capable of saturating the soil is usually lower in coarse-textured and shallower soils; analyzing landslide-triggering in clay soils, the authors in [104] observed a more rapid increase in the soil water potential (SWP), and a decrease in the corresponding safety factor, in a site with a lower soil depth. Furthermore, the higher hydraulic conductivity of coarser soils results in a faster raising of the wetting front, which reaches the bottom of the soil layer in a shorter amount of time, changing the zero-pore water pressure to a positive pressure, and destabilizing the slope. Andrewwinner et al. [105] used a finite-difference model to analyze a rainfall-triggered landslide that occurred on silty sand with a considerable amount of kaolinite clay, and identified a local rainfall threshold of a daily rainfall intensity of 142 mm without an antecedent rainfall. Alternatively, an antecedent rainfall of 151 mm within 5 consecutive days can initiate a landslide, where the failure increase in pore water pressure is due to prolonged rainfall. They also observed that the increase in the soil water pressure that causes the failure was enhanced by the presence of fine soil particles. Given the same textural class, the accumulation of organic matter in the soil profiles appears to exert a significant stabilizing effect. In a study investigating the influence of Alpine soil properties on shallow movements, Stanchi et al. (2012) [39] observed that topsoils (0–20 cm) were generally characterized by a better resistance to failure than subsoils (20–70 cm) due to their better plasticity, structure, and consistency, related to their organic binding agents, which can be affected by land management favoring organic matter input or conservation.

Hydromechanical models have been used to assess the site-specific slope stability and to predict critical combinations of groundwater levels, soil water content, and precipitation. However, such models for a slope stability evaluation require knowledge about the mechanical and hydraulic parameters of the soils, lithostratigraphy and morphology from the site characterization, and monitoring and laboratory tests [106]. Several recent studies aimed to improve the effectiveness of rainfall thresholds for landslides by considering the soil characteristics, such as soil depth or soil moisture [107–109]. The results of the present study showed that the information on soils that is already available in regional and national databases allows us to define rainfall thresholds more accurately than empirical thresholds based solely on the meteorological conditions leading to the triggering of shallow landslides.

The soil-based pedological thresholds were systematically lower, and in some cases significantly lower, than the reference curves, stressing the primary role of pedological conditioning factors in the activation of rainfall-induced shallow landslides and mud-debris

flows. This means that a considerable number of events may be missed when pedological conditioning factors are not considered in defining rainfall thresholds. Furthermore, the differentiated rainfall thresholds established for the separate soil regions, soil texture domains, and pedogenesis associated with organic matter accumulation highlighted significant differences in the responses of soils to the rainfall conditions that were able to trigger landslides.

5. Conclusions

Landslides are widespread natural processes that result from the contribution of several natural and anthropogenic factors. When occurring in populated areas, they represent hazards for property and lives. Several methodologies to define rainfall thresholds have been proposed in past decades to identify the relationship between precipitation and the triggering of shallow landslides in populated areas and to support early warning systems. In this study, in addition to the intensity–duration criteria, different rainfall thresholds were defined considering some of the pedological characteristics available in regional soil-related databases, such as the soil region, the textural class, and the STU. Based on an empirical approach, which uses a large dataset of shallow landslides in the Lombardy region, this research has obtained several inputs in relation to the declared aim.

(i) The study showed that among the soil characteristics examined, which were the topographic and precipitation characteristics of triggered landslides, the one most correlated with the characteristics of rainfall events was soil depth. Rainfall events that triggered landslides lasted longer when the soil was deeper; in contrast, short, high-intensity events seemed more likely to trigger landslides in shallow soils. The organic carbon content and the percentage of rock fragments were not significantly correlated with the characteristics of landslide-triggering events.

(ii) There were significant and positive correlations between the topographical characteristics (elevation and slope) and the stoniness and rockiness. The correlations between altitude and slope around the landslide sites and precipitation characteristics were not statistically significant. On the contrary, there were significant and positive correlations between topographical characteristics (in terms of slope and elevation) and stoniness and rockiness; in particular, where landslides were triggered along steeper slopes, the soils were shallower.

(iii) The soil-based rainfall thresholds for the Alps and Prealps of Lombardy obtained by considering the soil regions were significantly different, with a lower threshold for landslide occurrence in the soil region M1, with soil developed over siliceous parent material, with respect to the whole study area and the soil region M2, which was characterized by soils developed over calcareous bedrock. The Skeletic Cambisols, the most widespread soils in the study area, showed the highest landslide density in both the M1 and M2 regions. Furthermore, considering textural classes (fine and coarse), the curves were also differentiated, with coarse soils being more susceptible to the triggering of landslides than fine soils.

(iv) Considering both the texture and the main soil groups in the study area, given the same rainfall duration, the cumulative rainfall (and the rainfall intensity) needed to initiate a landslide increased in the following order: coarse and skeletal Cambisols < Umbrisols $\leq$ Podzols < fine Cambisols. The results of this study highlighted the primary role of pedological conditioning factors in differentiating the activation of rainfall-induced shallow landslides in a definite region.

(v) The information on soils that is already available in regional and national databases could be used to define rainfall-pedological thresholds more accurately than empirical thresholds based solely on meteorological conditions, even when they are locally defined, and can be used to improve the ability of early warning systems to forecast the occurrence of shallow landslides and mud-debris flows.

Further evaluation of the effectiveness of the soil-rainfall thresholds defined in the present study should be carried out, considering some real study cases, prior to their adoption in early-warning systems.

Author Contributions: Conceptualization, F.L. and L.T.; methodology, F.L., F.U. and L.T.; validation, F.F., J.D.G., A.R. and M.F.; formal analysis, L.T., M.B. and F.U.; investigation, F.L., M.B., L.T. and A.R.; resources, F.L. and L.T.; data curation, L.T., M.B. and A.R.; writing—original draft preparation, L.T., F.U., A.R., J.D.G. and M.B.; writing—review and editing, M.B., F.F., M.F. and M.D.; visualization, F.L., F.U. and L.T.; supervision, F.L. and L.T.; project administration, F.L. and L.T.; funding acquisition, F.L. All authors have read and agreed to the published version of the manuscript.

Funding: The research activity is financed by: DEBRIS FLOW Valcamonica CNR IRPI Project, supported by Lombardy region (Italy) Project CNR Number DTA. AD003599.

Institutional Review Board Statement: Not applicable.

Informed Consent Statement: Not applicable.

Data Availability Statement: The data presented in this study are available on request from the first author.

Conflicts of Interest: The authors declare no conflict of interest.

References

1. Bryant, E. *Natural Hazards*, 2nd ed.; Cambridge University Press: Cambridge, UK, 2005.
2. European Environment Agency. *Mapping the Impacts of Natural Hazards and Technological Accidents in Europe: An Overview of the Last Decade*; Publications Office of the European Union: Luxembourg, 2011.
3. Petley, D. Global Patterns of Loss of Life from Landslides. *Geology* **2012**, *40*, 927–930. [CrossRef]
4. Froude, M.J.; Petley, D.N. Global Fatal Landslide Occurrence from 2004 to 2016. *Nat. Hazards Earth Syst. Sci.* **2018**, *18*, 2161–2181. [CrossRef]
5. Haque, U.; da Silva, P.F.; Devoli, G.; Pilz, J.; Zhao, B.; Khaloua, A.; Wilopo, W.; Andersen, P.; Lu, P.; Lee, J.; et al. The Human Cost of Global Warming: Deadly Landslides and Their Triggers (1995–2014). *Sci. Total Environ.* **2019**, *682*, 673–684. [CrossRef]
6. Mărgărint, M.C.; Niculiţă, M. Landslide Type and Pattern in Moldavian Plateau, NE Romania. In *Landform Dynamics and Evolution in Romania*; Radoane, M., Vespremeanu-Stroe, A., Eds.; Springer Geography; Springer International Publishing: Cham, Switzerland, 2017; pp. 271–304. [CrossRef]
7. Popescu, M.E. Landslide Causal Factors and Landslide Remediatial Options. In Proceedings of the 3rd International Conference on Landslides, Slope Stability and Safety of Infra-Structures, Singapore, 11–12 July 2002; pp. 61–81.
8. Lukić, T.; Bjelajac, D.; Fitzsimmons, K.E.; Marković, S.B.; Basarin, B.; Mlađan, D.; Micić, T.; Schaetzl, R.J.; Gavrilov, M.B.; Milanović, M.; et al. Factors Triggering Landslide Occurrence on the Zemun Loess Plateau, Belgrade Area, Serbia. *Environ. Earth Sci.* **2018**, *77*, 519. [CrossRef]
9. Morar, C.; Lukić, T.; Basarin, B.; Valjarević, A.; Vujičić, M.; Niemets, L.; Telebienieva, I.; Boros, L.; Nagy, G. Shaping Sustainable Urban Environments by Addressing the Hydro-Meteorological Factors in Landslide Occurrence: Ciuperca Hill (Oradea, Romania). *Int. J. Environ. Res. Public. Health* **2021**, *18*, 5022. [CrossRef]
10. Crosta, G.B.; Frattini, P. Distributed Modelling of Shallow Landslides Triggered by Intense Rainfall. *Nat. Hazards Earth Syst. Sci.* **2003**, *3*, 81–93. [CrossRef]
11. Peruccacci, S.; Brunetti, M.T.; Luciani, S.; Vennari, C.; Guzzetti, F. Lithological and Seasonal Control on Rainfall Thresholds for the Possible Initiation of Landslides in Central Italy. *Geomorphology* **2012**, *139–140*, 79–90. [CrossRef]
12. Tiranti, D.; Nicolò, G.; Gaeta, A.R. Shallow Landslides Predisposing and Triggering Factors in Developing a Regional Early Warning System. *Landslides* **2019**, *16*, 235–251. [CrossRef]
13. Aleotti, P. A Warning System for Rainfall-Induced Shallow Failures. *Eng. Geol.* **2004**, *73*, 247–265. [CrossRef]
14. Baum, R.L.; Godt, J.W. Erratum to: Early Warning of Rainfall-Induced Shallow Landslides and Debris Flows in the USA. *Landslides* **2010**, *7*, 387. [CrossRef]
15. Papa, M.N.; Medina, V.; Ciervo, F.; Bateman, A. Derivation of Critical Rainfall Thresholds for Shallow Landslides as a Tool for Debris Flow Early Warning Systems. *Hydrol. Earth Syst. Sci.* **2013**, *17*, 4095–4107. [CrossRef]
16. Piciullo, L.; Gariano, S.L.; Melillo, M.; Brunetti, M.T.; Peruccacci, S.; Guzzetti, F.; Calvello, M. Definition and Performance of a Threshold-Based Regional Early Warning Model for Rainfall-Induced Landslides. *Landslides* **2017**, *14*, 995–1008. [CrossRef]
17. Segoni, S.; Rosi, A.; Rossi, G.; Catani, F.; Casagli, N. Analysing the Relationship between Rainfalls and Landslides to Define a Mosaic of Triggering Thresholds for Regional-Scale Warning Systems. *Nat. Hazards Earth Syst. Sci.* **2014**, *14*, 2637–2648. [CrossRef]
18. Revellino, P.; Hungr, O.; Guadagno, F.M.; Evans, S.G. Velocity and Runout Simulation of Destructive Debris Flows and Debris Avalanches in Pyroclastic Deposits, Campania Region, Italy. *Environ. Geol.* **2004**, *45*, 295–311. [CrossRef]
19. Huang, Y.; Sun, J.; Zhu, C. Mechanism and Prevention of Debris Flow Disaster. *Water* **2022**, *14*, 1143. [CrossRef]

20. He, S.; Liu, W.; Li, X. Prediction of Impact Force of Debris Flows Based on Distribution and Size of Particles. *Environ. Earth Sci.* **2016**, *75*, 298. [CrossRef]
21. House, P.K. Using Geology to Improve Flood Hazard Management on Alluvial Fans—An Example From Laughlin, Nevada. *J. Am. Water Resour. Assoc.* **2005**, *41*, 1431–1447. [CrossRef]
22. Chang, T.-C.; Wang, Z.-Y.; Chien, Y.-H. Hazard Assessment Model for Debris Flow Prediction. *Environ. Earth Sci.* **2010**, *60*, 1619–1630. [CrossRef]
23. Quan Luna, B.; Blahut, J.; Camera, C.; van Westen, C.; Apuani, T.; Jetten, V.; Sterlacchini, S. Physically Based Dynamic Run-out Modelling for Quantitative Debris Flow Risk Assessment: A Case Study in Tresenda, Northern Italy. *Environ. Earth Sci.* **2014**, *72*, 645–661. [CrossRef]
24. Turconi, L.; De, S.K.; Demurtas, F.; Demurtas, L.; Pendugiu, B.; Tropeano, D.; Savio, G. An Analysis of Debris-Flow Events in the Sardinia Island (Thyrrenian Sea, Italy). *Environ. Earth Sci.* **2013**, *69*, 1509–1521. [CrossRef]
25. Luino, F. Sequence of Instability Processes Triggered by Heavy Rainfall in the Northern Italy. *Geomorphology* **2005**, *66*, 13–39. [CrossRef]
26. Guzzetti, F.; Peruccacci, S.; Rossi, M.; Stark, C.P. The Rainfall Intensity–Duration Control of Shallow Landslides and Debris Flows: An Update. *Landslides* **2008**, *5*, 3–17. [CrossRef]
27. Segoni, S.; Piciullo, L.; Gariano, S.L. A Review of the Recent Literature on Rainfall Thresholds for Landslide Occurrence. *Landslides* **2018**, *15*, 1483–1501. [CrossRef]
28. Guzzetti, F. Landslide Fatalities and the Evaluation of Landslide Risk in Italy. *Eng. Geol.* **2000**, *58*, 89–107. [CrossRef]
29. Salvati, P.; Bianchi, C.; Rossi, M.; Guzzetti, F. Societal Landslide and Flood Risk in Italy. *Nat. Hazards Earth Syst. Sci.* **2010**, *10*, 465–483. [CrossRef]
30. Salvati, P.; Bianchi, C. *Rapporto Sul Rischio Posto Alla Popolazione Italiana da Frane e Inondazioni. Quinquennio 2014–2018*; CNR-IRPI: Perugia, Italy, 2019. Available online: https://polaris.irpi.cnr.it/report/ (accessed on 10 February 2022).
31. Govi, M.; Mortara, G.; Sorzana, P.F. Eventi Idrologici e Frane. *Geol. Appl. Idrogeol.* **1985**, *18*, 359–375.
32. Govi, M.; Turitto, O. *Ricerche Bibliografiche per Un Catalogo Sulle Inondazioni, Piene Torrentizie, Frane in Valtellina e Valchiavenna*; Quaderni di Studi e di Documentazione. Associazione Mineraria Subalpina, 1994. Available online: https://geomorphology.irpi.cnr.it (accessed on 10 February 2022).
33. Tropeano, D.; Govi, M.; Mortara, G.; Turitto, O.; Sorzana, P.F.; Negrini, G.; Arattano, M. *Eventi Alluvionali e Frane in Italia Settentrionale Nel Periodo 1975–1981*; L'Artistica Savigliano: Torino, Italy, 1999.
34. Tropeano, D.; Luino, F.; Turconi, L. *Eventi di Piena e Frana in Italia Settentrionale nel Periodo 2002–2004*; SMS: Bussoleno, Italy, 2006.
35. Turconi, L.; Luino, F. *Eventi di Piena e Frana in Italia Settentrionale nel Periodo 2005–2016*; SMS: Moncalieri, Italy, 2017.
36. Moser, M.; Hohensinn, F. Geotechnical Aspects of Soil Slips in Alpine Regions. *Eng. Geol.* **1983**, *19*, 185–211. [CrossRef]
37. Meusburger, K.; Alewell, C. Impacts of Anthropogenic and Environmental Factors on the Occurrence of Shallow Landslides in an Alpine Catchment (Urseren Valley, Switzerland). *Nat. Hazards Earth Syst. Sci.* **2008**, *8*, 509–520. [CrossRef]
38. Norbiato, D.; Borga, M.; Merz, R.; Blöschl, G.; Carton, A. Controls on Event Runoff Coefficients in the Eastern Italian Alps. *J. Hydrol.* **2009**, *375*, 312–325. [CrossRef]
39. Stanchi, S.; Freppaz, M.; Zanini, E. The Influence of Alpine Soil Properties on Shallow Movement Hazards, Investigated through Factor Analysis. *Nat. Hazards Earth Syst. Sci.* **2012**, *12*, 1845–1854. [CrossRef]
40. Stanchi, S.; Freppaz, M.; Oberto, E.; Caimi, A.; Zanini, E. Plastic and Liquid Limits in Alpine Soils: Methods of Measurement and Relations with Soil Properties. *Adv. Geoecol.* **2008**, *39*, 594–604.
41. Peruccacci, S.; Brunetti, M.T.; Gariano, S.L.; Melillo, M.; Rossi, M.; Guzzetti, F. Rainfall Thresholds for Possible Landslide Occurrence in Italy. *Geomorphology* **2017**, *290*, 39–57. [CrossRef]
42. Palladino, M.R.; Viero, A.; Turconi, L.; Brunetti, M.T.; Peruccacci, S.; Melillo, M.; Luino, F.; Deganutti, A.M.; Guzzetti, F. Rainfall Thresholds for the Activation of Shallow Landslides in the Italian Alps: The Role of Environmental Conditioning Factors. *Geomorphology* **2018**, *303*, 53–67. [CrossRef]
43. Roccati, A.; Faccini, F.; Luino, F.; Ciampalini, A.; Turconi, L. Heavy Rainfall Triggering Shallow Landslides: A Susceptibility Assessment by a GIS-Approach in a Ligurian Apennine Catchment (Italy). *Water* **2019**, *11*, 605. [CrossRef]
44. Guzzetti, F.; Peruccacci, S.; Rossi, M.; Stark, C.P. Rainfall Thresholds for the Initiation of Landslides in Central and Southern Europe. *Meteorol. Atmos. Phys.* **2007**, *98*, 239–267. [CrossRef]
45. Zêzere, J.L. Landslide Susceptibility Assessment Considering Landslide Typology. A Case Study in the Area North of Lisbon (Portugal). *Nat. Hazards Earth Syst. Sci.* **2002**, *2*, 73–82. [CrossRef]
46. Abraham, M.T.; Pothuraju, D.; Satyam, N. Rainfall Thresholds for Prediction of Landslides in Idukki, India: An Empirical Approach. *Water* **2019**, *11*, 2113. [CrossRef]
47. Jordanova, G.; Gariano, S.L.; Melillo, M.; Peruccacci, S.; Brunetti, M.T.; Jemec Auflič, M. Determination of Empirical Rainfall Thresholds for Shallow Landslides in Slovenia Using an Automatic Tool. *Water* **2020**, *12*, 1449. [CrossRef]
48. Caine, N. The Rainfall Intensity: Duration Control of Shallow Landslides and Debris Flows. *Geogr. Ann. Ser. Phys. Geogr.* **1980**, *62*, 23. [CrossRef]
49. Wieczorek, G.F. Effect of Rainfall Intensity and Duration on Debris Flows in Central Santa Cruz Mountains, California. In *Reviews in Engineering Geology*; Geological Society of America: Boulder, CO, USA, 1987; Volume 7, pp. 93–104. [CrossRef]

50. Crosta, G. Regionalization of Rainfall Thresholds: An Aid to Landslide Hazard Evaluation. *Environ. Geol.* **1998**, *35*, 131–145. [CrossRef]
51. Saito, H.; Nakayama, D.; Matsuyama, H. Relationship between the Initiation of a Shallow Landslide and Rainfall Intensity—Duration Thresholds in Japan. *Geomorphology* **2010**, *118*, 167–175. [CrossRef]
52. Hong, M.; Kim, J.; Jeong, S. Rainfall Intensity-Duration Thresholds for Landslide Prediction in South Korea by Considering the Effects of Antecedent Rainfall. *Landslides* **2018**, *15*, 523–534. [CrossRef]
53. Roccati, A.; Faccini, F.; Luino, F.; Turconi, L.; Guzzetti, F. Rainfall Events with Shallow Landslides in the Entella Catchment, Liguria, Northern Italy. *Nat. Hazards Earth Syst. Sci.* **2018**, *18*, 2367–2386. [CrossRef]
54. Schultz, A.P.; Jibson, R.W. (Eds.) *Landslide Processes of the Eastern United States and Puerto Rico*; Special paper; Geological Society of America: Boulder, CO, USA, 1989.
55. Crosta, G.B.; Frattini, P. Rainfall Thresholds for Triggering Soil Slips and Debris Flow. In Proceedings of the 2nd EGS Plinius Conference on Mediterranean Storms, Siena, Italy, 16–18 October 2001; pp. 463–487.
56. Floris, M.; Mari, M.; Romeo, R.W.; Gori, U. Modelling of Landslide-Triggering Factors—A Case Study in the Northern Apennines, Italy. In *Engineering Geology for Infrastructure Planning in Europe*; Hack, R., Azzam, R., Charlier, R., Eds.; Lecture Notes in Earth Sciences; Springer: Berlin/Heidelberg, Germany, 2004; Volume 104, pp. 745–753. [CrossRef]
57. Brunetti, M.T.; Peruccacci, S.; Rossi, M.; Luciani, S.; Valigi, D.; Guzzetti, F. Rainfall Thresholds for the Possible Occurrence of Landslides in Italy. *Nat. Hazards Earth Syst. Sci.* **2010**, *10*, 447–458. [CrossRef]
58. Rosi, A.; Peternel, T.; Jemec-Auflič, M.; Komac, M.; Segoni, S.; Casagli, N. Rainfall Thresholds for Rainfall-Induced Landslides in Slovenia. *Landslides* **2016**, *13*, 1571–1577. [CrossRef]
59. Crozier, M.J. Prediction of Rainfall-Triggered Landslides: A Test of the Antecedent Water Status Model. *Earth Surf. Process. Landf.* **1999**, *24*, 825–833. [CrossRef]
60. Glade, T.; Crozier, M.; Smith, P. Applying Probability Determination to Refine Landslide-Triggering Rainfall Thresholds Using an Empirical "Antecedent Daily Rainfall Model". *Pure Appl. Geophys.* **2000**, *157*, 1059–1079. [CrossRef]
61. Godt, J.W.; Baum, R.L.; Lu, N. Landsliding in Partially Saturated Materials: Landslide Forecasting. *Geophys. Res. Lett.* **2009**, *36*, L02403. [CrossRef]
62. Bogaard, T.; Greco, R. Invited Perspectives: Hydrological Perspectives on Precipitation Intensity-Duration Thresholds for Landslide Initiation: Proposing Hydro-Meteorological Thresholds. *Nat. Hazards Earth Syst. Sci.* **2018**, *18*, 31–39. [CrossRef]
63. Valenzuela, P.; Domínguez-Cuesta, M.J.; Mora García, M.A.; Jiménez-Sánchez, M. Rainfall Thresholds for the Triggering of Landslides Considering Previous Soil Moisture Conditions (Asturias, NW Spain). *Landslides* **2018**, *15*, 273–282. [CrossRef]
64. Zhao, B.; Dai, Q.; Han, D.; Dai, H.; Mao, J.; Zhuo, L. Probabilistic Thresholds for Landslides Warning by Integrating Soil Moisture Conditions with Rainfall Thresholds. *J. Hydrol.* **2019**, *574*, 276–287. [CrossRef]
65. Bogaard, T.A.; van Asch, T.W.J. The Role of the Soil Moisture Balance in the Unsaturated Zone on Movement and Stability of the Beline Landslide, France. *Earth Surf. Process. Landf.* **2002**, *27*, 1177–1188. [CrossRef]
66. Salciarini, D.; Godt, J.W.; Savage, W.Z.; Conversini, P.; Baum, R.L.; Michael, J.A. Modeling Regional Initiation of Rainfall-Induced Shallow Landslides in the Eastern Umbria Region of Central Italy. *Landslides* **2006**, *3*, 181–194. [CrossRef]
67. Zung, A.B.; Sorenson, C.J.; Winthers, E. Landslide Soils and Geomorphology in Bridger-Teton National Forest, Northwest Wyoming. *Phys. Geogr.* **2009**, *30*, 501–516. [CrossRef]
68. Li, G.; Lei, Y.; Yao, H.; Wu, S.; Ge, J. The Influence of Land Urbanization on Landslides: An Empirical Estimation Based on Chinese Provincial Panel Data. *Sci. Total Environ.* **2017**, *595*, 681–690. [CrossRef]
69. Persichillo, M.G.; Bordoni, M.; Meisina, C. The Role of Land Use Changes in the Distribution of Shallow Landslides. *Sci. Total Environ.* **2017**, *574*, 924–937. [CrossRef]
70. Tofani, V.; Bicocchi, G.; Rossi, G.; Segoni, S.; D'Ambrosio, M.; Casagli, N.; Catani, F. Soil Characterization for Shallow Landslides Modeling: A Case Study in the Northern Apennines (Central Italy). *Landslides* **2017**, *14*, 755–770. [CrossRef]
71. Montgomery, D.R.; Dietrich, W.E. A Physically Based Model for the Topographic Control on Shallow Landsliding. *Water Resour. Res.* **1994**, *30*, 1153–1171. [CrossRef]
72. Iverson, R.M. Landslide Triggering by Rain Infiltration. *Water Resour. Res.* **2000**, *36*, 1897–1910. [CrossRef]
73. Tsaparas, I.; Rahardjo, H.; Toll, D.G.; Leong, E.C. Controlling Parameters for Rainfall-Induced Landslides. *Comput. Geotech.* **2002**, *29*, 1–27. [CrossRef]
74. Rosso, R.; Rulli, M.C.; Vannucchi, G. A Physically Based Model for the Hydrologic Control on Shallow Landsliding: Hydrologic control on shallow landsliding. *Water Resour. Res.* **2006**, *42*, W06410. [CrossRef]
75. Tsai, T.-L.; Yang, J.-C. Modeling of Rainfall-Triggered Shallow Landslide. *Environ. Geol.* **2006**, *50*, 525–534. [CrossRef]
76. Anagnostopoulos, G.G.; Fatichi, S.; Burlando, P. An Advanced Process-Based Distributed Model for the Investigation of Rainfall-Induced Landslides: The Effect of Process Representation and Boundary Conditions: Modeling rainfall-induced landslides. *Water Resour. Res.* **2015**, *51*, 7501–7523. [CrossRef]
77. Schilirò, L.; Montrasio, L.; Scarascia Mugnozza, G. Prediction of Shallow Landslide Occurrence: Validation of a Physically-Based Approach through a Real Case Study. *Sci. Total Environ.* **2016**, *569–570*, 134–144. [CrossRef]
78. Chiu, Y.-Y.; Chen, H.-E.; Yeh, K.-C. Investigation of the Influence of Rainfall Runoff on Shallow Landslides in Unsaturated Soil Using a Mathematical Model. *Water* **2019**, *11*, 1178. [CrossRef]

79. Fan, L.; Lehmann, P.; Or, D. Effects of Soil Spatial Variability at the Hillslope and Catchment Scales on Characteristics of Rainfall-Induced Landslides: Soil spatial variability and rainfall-induced landslides. *Water Resour. Res.* **2016**, *52*, 1781–1799. [CrossRef]
80. Govi, M.; Sorzana, P.F. Landslide Susceptibility as a Function of Critical Rainfall Amount in Piedmont Basin (Northwestern Italy). *Stud. Geomorphol. Carpatho-Balc.* **1980**, *14*, 43–61.
81. Luino, F.; De Graff, J.; Roccati, A.; Biddoccu, M.; Cirio, C.G.; Faccini, F.; Turconi, L. Eighty Years of Data Collected for the Determination of Rainfall Threshold Triggering Shallow Landslides and Mud-Debris Flows in the Alps. *Water* **2019**, *12*, 133. [CrossRef]
82. Simoni, S.; Zanotti, F.; Bertoldi, G.; Rigon, R. Modelling the Probability of Occurrence of Shallow Landslides and Channelized Debris Flows Using GEOtop-FS. *Hydrol. Process.* **2008**, *22*, 532–545. [CrossRef]
83. Marazzi, S. Atlante Orografico Delle Alpi: SOIUSA, Suddivisione Orografica Internazionale Unificata Del Sistema Alpino. 2005. Available online: webgis.arpa.piemonte.it (accessed on 13 December 2021).
84. Ceriani, M.; Carelli, M. Carta Delle Precipitazioni Medie, Minime e Massime Annue Del Territorio Alpino Lombardi (Registrate Nel Periodo 1891–1990). 1992. Available online: http://www.centrometeolombardo.com/ (accessed on 13 December 2021).
85. Marra, F.; Nikolopoulos, E.I.; Creutin, J.D.; Borga, M. Space–Time Organization of Debris Flows-Triggering Rainfall and Its Effect on the Identification of the Rainfall Threshold Relationship. *J. Hydrol.* **2016**, *541*, 246–255. [CrossRef]
86. Fratianni, S.; Acquaotta, F. The Climate of Italy. In *Landscapes and Landforms of Italy*; Soldati, M., Marchetti, M., Eds.; World Geomorphological Landscapes; Springer International Publishing: Cham, Switzerland, 2017; pp. 29–38. [CrossRef]
87. Costantini, E.A.C.; L'Abate, G.; Barbetti, R.; Fantappié, M.; Lorenzetti, R.; Magini, S. Carta dei suoli d'Italia-Soil Map of Italy at 1:1,000,000 Scale. 2012, Consiglio per Ricerca e la Sperimentazione in Agricoltura, Ministero delle Politiche Agricole Alimentari e Forestali. Available online: https://esdac.jrc.ec.europa.eu/content/carta-dei-suoli-ditalia-soil-map-italy (accessed on 13 December 2021).
88. IUSS Working Group WRB. *Ld Reference Base for Soil Resources 2014, Update 2015: International Soil Classification System for Naming Soils and Creating Legends for Soil Maps*; World Soil Resources Report No. 106; Food and Agriculture Organization: Rome, Italy, 2015; 192p.
89. Brunetti, M.T.; Peruccacci, S.; Antronico, L.; Bartolini, D.; Deganutti, A.M.; Gariano, S.L.; Iovine, G.; Luciani, S.; Luino, F.; Melillo, M.; et al. Catalogue of Rainfall Events with Shallow Landslides and New Rainfall Thresholds in Italy. In *Engineering Geology for Society and Territory*; Lollino, G., Giordan, D., Crosta, G.B., Corominas, J., Azzam, R., Wasowski, J., Sciarra, N., Eds.; Springer International Publishing: Cham, Switzerland, 2015; Volume 2, pp. 1575–1579. [CrossRef]
90. Brenna, S.; D'Alessio, M.; Rasio, R. *Carta Dei Pedopaesaggi Della Lombardia—Pedo-Landscape Map of Lombardy. (Scale 1:250,000)*; Regione Lombardia; Agricoltura, Ente Regionale di Sviluppo Agricolo della Lombardia: Milano, Italy, 2001.
91. ERSAF. Basi Informative Dei Suoli. 2013. Available online: https://www.ersaf.lombardia.it/it (accessed on 15 September 2020).
92. ERSAF. I Suoli Della Lombardia. 2021. Available online: https://www.ersaf.lombardia.it/it (accessed on 15 September 2020).
93. Ledl, T. Kernel Density Estimation: Theory and Application in Discriminant Analysis. *Austrian J. Stat.* **2016**, *33*, 267–279. [CrossRef]
94. Silverman, B.W. *Density Estimation for Statistics and Data Analysis*, 1st ed.; Routledge: London, UK, 2018. [CrossRef]
95. Sheather, S.J. Density Estimation. *Stat. Sci.* **2004**, *19*, 588–597. [CrossRef]
96. Ceriani, M.; Lauzi, S.; Padovan, N. Rainfall Thresholds Triggering Debris Flows in the Alpine Area of Lombardia Region, Central Alps–Italy. In Proceedings of the Man and Mountain'94. First International Congress for the Protection and Development of Mountain Environment, Ponte di Legno, Italy, 20–24 June 1994; pp. 123–139.
97. Cancelli, A.; Nova, R. Landslide in Soil Debris Cover Triggered by Rainstorm in Valtellina. In Proceedings of the IV International Conference and Field Workshop on Landslides, Tokyo, Japan, 23–31 August 1985; pp. 267–272.
98. European Commission-European Soil Bureau Network. Soil Atlas of Europe. 2005. Available online: https://esdac.jrc.ec.europa.eu/content/soil-atlas-europe (accessed on 15 September 2020).
99. Gautam, P.; Kubota, T.; Sapkota, L.M.; Shinohara, Y. Landslide Susceptibility Mapping with GIS in High Mountain Area of Nepal: A Comparison of Four Methods. *Environ. Earth Sci.* **2021**, *80*, 359. [CrossRef]
100. Dapporto, S.; Aleotti, P.; Casagli, N.; Polloni, G. Analysis of Shallow Failures Triggered by the 14–16 November 2002 Event in the Albaredo Valley, Valtellina (Northern Italy). *Adv. Geosci.* **2005**, *2*, 305–308. [CrossRef]
101. Johnson, K.A.; Sitar, N. Hydrologic Conditions Leading to Debris-Flow Initiation. *Can. Geotech. J.* **1990**, *27*, 789–801. [CrossRef]
102. Fredlund, D.G.; Xing, A.; Fredlund, M.D.; Barbour, S.L. The Relationship of the Unsaturated Soil Shear Strength to the Soil-Water Characteristic Curve. *Can. Geotech. J.* **1996**, *33*, 440–448. [CrossRef]
103. Jotisankasa, A.; Vathananukij, H. Investigation of Soil Moisture Characteristics of Landslide-Prone Slopes in Thailand. In Proceedings of the International Conference on Management of Landslide Hazard in the Asia-Pacific Region, Sendai, Japan, 11–15 November 2008; p. 12.
104. Bordoni, M.; Inzaghi, F.; Vivaldi, V.; Valentino, R.; Bittelli, M.; Meisina, C. A Data-Driven Method for the Temporal Estimation of Soil Water Potential and Its Application for Shallow Landslides Prediction. *Water* **2021**, *13*, 1208. [CrossRef]
105. Andrewwinner, R.; Chandrasekaran, S.S. Investigation on the Failure Mechanism of Rainfall-Induced Long-Runout Landslide at Upputhode, Kerala State of India. *Land* **2021**, *10*, 1212. [CrossRef]

106. Moradi, S.; Heinze, T.; Budler, J.; Gunatilake, T.; Kemna, A.; Huisman, J.A. Combining Site Characterization, Monitoring and Hydromechanical Modeling for Assessing Slope Stability. *Land* **2021**, *10*, 423. [CrossRef]
107. Fusco, F.; Mirus, B.; Baum, R.; Calcaterra, D.; De Vita, P. Incorporating the Effects of Complex Soil Layering and Thickness Local Variability into Distributed Landslide Susceptibility Assessments. *Water* **2021**, *13*, 713. [CrossRef]
108. Sajinkumar, K.S.; Rinu, S.; Oommen, T.; Vishnu, C.L.; Praveen, K.R.; Rani, V.R.; Muraleedharan, C. Improved Rainfall Threshold for Landslides in Data Sparse and Diverse Geomorphic Milieu: A Cluster Analysis Based Approach. *Nat. Hazards* **2020**, *103*, 639–657. [CrossRef]
109. Marino, P.; Peres, D.J.; Cancelliere, A.; Greco, R.; Bogaard, T.A. Soil Moisture Information Can Improve Shallow Landslide Forecasting Using the Hydrometeorological Threshold Approach. *Landslides* **2020**, *17*, 2041–2054. [CrossRef]